

UNCLASSIFIED

AD NUMBER

AD602858

LIMITATION CHANGES

TO:

Approved for public release; distribution is unlimited.

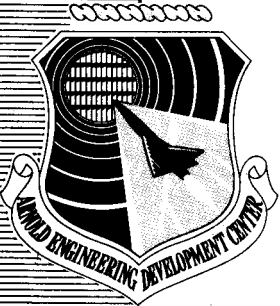
FROM:

Distribution authorized to U.S. Gov't. agencies and their contractors;  
Administrative/Operational Use; JUL 1964. Other requests shall be referred to Air Force Arnold Engineering Development Center, Arnold AFB, TN.

AUTHORITY

per dtic form 55

THIS PAGE IS UNCLASSIFIED



**CALCULATION OF THE  
D-C ELECTRICAL CONDUCTIVITY  
OF EQUILIBRIUM NITROGEN AND ARGON PLASMA  
WITH AND WITHOUT ALKALI METAL SEED**

**By**

**Lt. R.E. Weber, USAF, and K. E. Tempelmeyer  
Propulsion Wind Tunnel Facility  
ARO, Inc.**

**TECHNICAL DOCUMENTARY REPORT NO. AEDC-TDR-64-119**

**July 1964**

**Program Element 62410034/7778, Task 777805**

**(Prepared under Contract No. AF 40(600)-1000 by ARO, Inc.,  
contract operator of AEDC, Arnold Air Force Station, Tenn.)**

**ARNOLD ENGINEERING DEVELOPMENT CENTER  
AIR FORCE SYSTEMS COMMAND  
UNITED STATES AIR FORCE**

# ***NOTICES***

Qualified requesters may obtain copies of this report from DDC, Cameron Station, Alexandria, Va. Orders will be expedited if placed through the librarian or other staff member designated to request and receive documents from DDC.

When Government drawings, specifications or other data are used for any purpose other than in connection with a definitely related Government procurement operation, the United States Government thereby incurs no responsibility nor any obligation whatsoever; and the fact that the Government may have formulated, furnished, or in any way supplied the said drawings, specifications, or other data, is not to be regarded by implication or otherwise as in any manner licensing the holder or any other person or corporation, or conveying any rights or permission to manufacture, use, or sell any patented invention that may in any way be related thereto.

CALCULATION OF THE  
D-C ELECTRICAL CONDUCTIVITY  
OF EQUILIBRIUM NITROGEN AND ARGON PLASMA  
WITH AND WITHOUT ALKALI METAL SEED

By

Lt. R. E. Weber, USAF, and K. E. Tempelmeyer

Propulsion Wind Tunnel Facility

ARO, Inc.

a subsidiary of Sverdrup and Parcel, Inc.

ARO Project No. 2287

July 1964

## FOREWORD

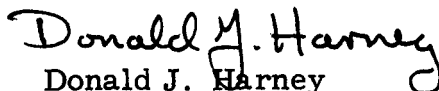
The authors gratefully acknowledge the assistance of R. L. Sanders who programmed an electronic computer and obtained the numerical calculations presented here, and the assistance of W. L. Powers in the derivation of the matrix equation contained in Appendix III. Also, the authors would like to thank G. Huggins who assisted in many ways during the course of the work described here.

**ABSTRACT**

Scalar electrical conductivities have been computed for nitrogen and argon plasma in thermal equilibrium. Calculations have been made for these gases both unseeded and seeded with cesium, potassium, and NaK in amounts ranging from 0.01 to 10 percent seed by weight, and cover a range of pressure and temperature from  $10^{-2}$  to  $10^3$  atm and from 2000 to 15,000°K, respectively. Calculated electrical conductivities are presented in figure form as a function of temperature with seed rate and pressure as parameters. Some effects of applied magnetic fields up to 20,000 gauss on the conductivity of potassium-seeded nitrogen are also given.

**PUBLICATION REVIEW**

This report has been reviewed and publication is approved.

  
Donald J. Harney  
Major, USAF  
Chief, Special Projects Office  
DCS/Civil Engineering

  
Donald R. Eastman, Jr.  
DCS/Research

## CONTENTS

	<u>Page</u>
ABSTRACT. . . . .	v
NOMENCLATURE. . . . .	ix
1.0 INTRODUCTION . . . . .	1
2.0 SCALAR ELECTRICAL CONDUCTIVITY	
2.1 Conductivity Equations . . . . .	1
2.2 Collision Cross Sections . . . . .	4
2.3 Calculation of Number Density . . . . .	5
3.0 CALCULATION OF ELECTRICAL CONDUCTIVITY WITH MAGNETIC FIELDS	
3.1 Tensor Conductivity Equations . . . . .	8
3.2 Ion-Neutral Cross Sections . . . . .	13
4.0 NUMERICAL COMPUTATIONS	
4.1 Scalar Conductivity . . . . .	14
4.2 Tensor Conductivity. . . . .	16
4.3 Validity of Calculations . . . . .	16
REFERENCES . . . . .	17
APPENDICES	
I. Calculation of Particle Densities for Seeded Argon . . . . .	21
II. Calculation of Particle Densities for Seeded Nitrogen . . . . .	24
III. Tensor Conductivity Equations. . . . .	27

## TABLES

1. Number Fractions of Equilibrium Nitrogen. . . . .	31
2. Typical Values of $\ln \Lambda$ for Nitrogen. . . . .	33

## ILLUSTRATIONS

Figure

1. Calculated Electron-Ion Collision Cross Sections for Argon . . . . .	35
2. Electron-Neutral Collision Cross Section for Argon . . . . .	36

<u>Figure</u>		<u>Page</u>
3.	Comparison of Collision Cross Sections for Nitrogen	
	a. N <sub>2</sub> -e. . . . .	37
	b. N-e . . . . .	37
4.	Experimental Electron-Neutral Elastic Collision Cross Sections (Ref. 32). . . . .	38
5.	Ionization Equilibrium Constant Function for Selected Elements. . . . .	39
6.	Experimental Ion-Neutral Collision Cross Sections for Various Substances (Ref. 22)	
	a. Ions in Argon. . . . .	40
	b. Potassium Ions in Nitrogen. . . . .	40
7.	Equilibrium Electrical Conductivities of Unseeded Argon	
	a. With Ref. 25 Cross Sections . . . . .	41
	b. With Ref. 22 Cross Sections . . . . .	41
8.	Equilibrium Electrical Conductivity of Argon Seeded with Various Amounts of Cesium . . . . .	42
9.	Equilibrium Electrical Conductivity of Argon Seeded with Various Amounts of Potassium. . . . .	43
10.	Equilibrium Electrical Conductivity of Unseeded Nitrogen. . . . .	44
11.	Equilibrium Electrical Conductivity of Nitrogen Seeded with Various Amounts of Cesium. . . . .	45
12.	Equilibrium Electrical Conductivity of Nitrogen Seeded with Various Amounts of Potassium . . . . .	46
13.	Equilibrium Electrical Conductivity of Nitrogen Seeded with Various Amounts of NaK . . . . .	47
14.	Typical Values of the Hall Parameter, $\omega_e \bar{\tau}_e$ . . . . .	48
15.	Typical Values of the Ion-Slip Factor . . . . .	49
16.	Effect of a Magnetic Field on Electrical Conductivity of Nitrogen Seeded with 0.1 percent Potassium	
	a. p = 0.10 atm . . . . .	50
	b. p = 1.00 atm . . . . .	51
17.	Effect of a Magnetic Field on Electrical Conductivity of Nitrogen Seeded with 1.0 percent Potassium	
	a. p = 0.10 atm . . . . .	52
	b. p = 1.00 atm . . . . .	53



## NOMENCLATURE

B	Magnetic flux density, weber/m <sup>2</sup>
b	Ion-slip factor defined following Eq. (24)
C	Seeding rate factor defined by Eq. (13)
E	Electric field, volt/m
E'	Effective electric field ( $\vec{E} + \vec{V} \times \vec{B}$ ), volt/m
e	Electronic charge, $1.602 \times 10^{-19}$ , coulomb
f	Fraction of neutral particles, $(1 - \phi)$
h	Planck's constant, $6.62 \times 10^{-34}$ , joule-sec
I <sub>p</sub>	Ionization potential, joule
$\vec{i}, \vec{j}, \vec{k}$	Unit vectors
J	Current density, amp/m <sup>2</sup>
K	Equilibrium constant, 1/m <sup>3</sup>
k	Boltzmann constant, $1.380 \times 10^{-23}$ , joule/°K
M	Molecular weight, kg/(kg-mole)
m	Particle mass, kg
No	Avogadro's number, $6.025 \times 10^{26}$
n	Number density, number/m <sup>3</sup>
p	Pressure, newton/m <sup>2</sup> or atm (1 atm = $1.013 \times 10^5$ newton/m <sup>2</sup> )
Q	Collision cross section, m <sup>2</sup>
R	Gas constant, $8.314 \times 10^3$ , joule/(kg-mole) °K
S	Seeding rate (ratio of weight of seed to total mixture weight)
T	Temperature, °K
V	Velocity, m/sec
$\bar{v}$	Mean particle velocity, m/sec
X	Molar fraction
Y	Mass fraction
Z	Partition function
$\beta$	Defined by Eq. (22)

$\epsilon_0$	Permittivity of free space, $10^{-9}/36\pi$ , farad/m
$\kappa$	Defined by Eq. (21)
$\Lambda$	Ratio of Debye length to impact parameter defined by Eq. (3)
$\sigma$	Scalar equilibrium electrical conductivity, mho/m
$\sigma_{\text{eff}}$	Effective tensor conductivity, mho/m
$\tau$	Mean free time between collisions, sec
$\bar{\tau}$	Effective mean free time defined after Eq. (24), sec
$\phi$	Fraction of ionized particles
$\omega$	Cyclotron frequency, 1/sec

#### SUBSCRIPTS

A	Argon or applied
Cs	Cesium
e	Electron
eff	Effective
ei	Electron-ion
ej	Electron-specie
en	Electron-neutral
f	Fully ionized
g	Gas
H	Hall
i	Ion or induced
in	Ion-neutral
j	Specie index
m	Mixture after ionization
N	Nitrogen atom
N <sub>2</sub>	Nitrogen molecule
n	Neutral
s	Seed
T	Total
w	Weakly Ionized
x, y, z	Orthogonal co-ordinates

## 1.0 INTRODUCTION

Because of recent research into magnetohydrodynamic (MHD) power generation and plasma acceleration, there has been an increasing effort to determine the electrical conductivity of gaseous plasmas. A knowledge of the conductivity is essential for the interpretation of MHD experimental phenomena or for making realistic predictions from theory. Calculated values of scalar d-c electrical conductivities are available for a few gases (see Refs. 1 through 6 for example). Also, several investigators have attempted to measure electrical conductivities but usually over a limited temperature range and below 2500°K. References 7 through 15 summarize most of the available experimental data which, in general, have been obtained for air and seeded combustion gases.

As part of an experimental investigation of a steady-flow, crossed-field, d-c accelerator at Arnold Engineering Development Center (AEDC), Air Force Systems Command (AFSC), additional computations of equilibrium scalar conductivities have been made for nitrogen and argon both unseeded and seeded with cesium (Cs), potassium (K), and NaK (a eutectic mixture of sodium and potassium). The results of these calculations which cover a temperature range from 2000 to 15,000°K and pressures from 0.01 to 10 atm are presented here. For unseeded argon, however, the results of some additional calculations are given for pressures up to  $10^3$  atm.

Application of a magnetic field to a plasma gives rise to electric fields and currents in various directions; for example, the Hall field, and as a result the conductivity becomes a tensor quantity. Sonnerup analyzes this effect (Ref. 16) and Brunner (Ref. 1) has made some calculations to show the significance of tensor conductivity in air. Some additional calculations of the three primary tensor components of the conductivity induced by magnetic fields from 5000 to 20,000 gauss (that is, 0.5 to 2.0 weber/m<sup>2</sup>) in seeded nitrogen are also presented.

Application of an electric field to a plasma can result in the electrons being selectively heated, and the conductivity becomes a function of the applied field. Kerrebrock (Refs. 17 and 18) has termed this phenomenon "non-equilibrium conductivity." No attempt has been made to account for this effect in any of the calculations reported here.

## 2.0 SCALAR ELECTRICAL CONDUCTIVITY

### 2.1 CONDUCTIVITY EQUATIONS

Theories for predicting electrical conductivities in gases have been developed for the two extreme cases of weakly ionized gases and fully

---

Manuscript received May 1964.

ionized gases. In both cases the analysis assumes thermal equilibrium ( $T_n = T_i = T_e$ ) and single ionizations ( $n_e = n_i$ ).

Chapman and Cowling (Ref. 19) have made a careful analysis for weakly ionized gases in which they consider binary collisions between neutral particles and electrons; that is, since  $n_i \ll n_n$  they only take close encounters into account. The Chapman and Cowling conductivity expression may be written

$$\sigma_w = \frac{0.532 n_e e^2}{(m_e kT)^{1/2}} \left( \frac{1}{n_n Q_{en}} \right) \quad (1)$$

Several theoretical approaches have been used to derive expressions for the conductivity of fully ionized gases, but the formula derived by Spitzer and Härm (Ref. 20) is most universally accepted. Because  $n_n = 0$  for fully ionized gases, only distant encounters are considered. For fully ionized gases, Spitzer-Härm obtain

$$\sigma_f = 0.591 (4\pi \epsilon_0)^2 \frac{(kT)^{3/2}}{m_e^{1/2} e^2} \frac{1}{\ln \Lambda} \quad (2)$$

where

$$\Lambda = \frac{12\pi}{e^3} \left[ \frac{(\epsilon_0 kT)^3}{2 n_e} \right]^{1/2} \quad (3)$$

is the ratio of the Debye length to an impact parameter for a 90-deg deflection of the electron by the ion.

The ranges over which these conductivity theories are believed to provide reasonably accurate results depend on several factors, but roughly the Chapman and Cowling equation is useful at temperatures below 3000 to 4000°K and the Spitzer-Härm equation at temperatures above 10,000 to 12,000°K. No fundamental theory founded on basic principles is known to exist in the intermediate range, which is referred to hereafter as a partially ionized gas. However, an approximate equation for the electrical conductivity of a plasma having an arbitrary degree of ionization has been proposed by Lin, Resler, and Kantrowitz (Ref. 8). They have argued that the electrical resistances caused by neutral particles and ionized particles should be additive, and thus,

$$\frac{1}{\sigma} = \frac{1}{\sigma_w} + \frac{1}{\sigma_f} \quad (4)$$

This simple formula appears to provide reasonable results and is used widely in computations of  $\sigma$ .

Although there is some doubt in regard to defining cross sections for charged particles based on the concept of binary collisions, Lin, Resler,

and Kantrowitz note that the Spitzer-Härm equation, Eq. (2), assumes the same form as the Chapman-Cowling equation, Eq. (1), if one defines an effective ion-electron cross section as

$$Q_{ei} = \frac{0.9 e^4}{(4 \pi \epsilon_0 kT)^2} \ln \left\{ \frac{12 \pi}{e^3} \left[ \frac{(\epsilon_0 kT)^3}{2 n_e} \right]^{1/2} \right\} \quad (5)$$

Combination of Eqs. (1) through (5) results in an expression for the electrical conductivity for monatomic gases,

$$\sigma = \frac{0.532 n_e e^2}{m_e^{1/2} (kT)^{1/2}} \left[ n_n Q_{en} + n_i Q_{ei} \right]^{-1} \quad (6)$$

This equation has been further generalized to allow the calculation of the conductivities of more complicated gases and seeded gases. In a slightly more general form, Eq. (6) may be written,

$$\sigma = \frac{0.532 n_e e^2}{m_e^{1/2} (kT)^{1/2}} \left( \sum n_j Q_{ej} \right)^{-1} \quad (7)$$

Equation (7), except for the numerical coefficient, can also be derived by the so-called "free-path kinetic theory" in which it is assumed that the particles make instantaneous collisions with each other but move freely between collisions. This derivation is discussed in more detail by Sherman (Ref. 21). The summation term represents the electron mean free path for gaseous mixtures.

Additional terms are added to the summation to account for collisions contributed by the various seed particles and the various gas species. For example, for cesium-seeded nitrogen Eq. (7) would be

$$\sigma = \frac{0.532 n_e e^2}{m_e^{1/2} (kT)^{1/2}} \left( n_{N_2} Q_{N_2-e} + n_N Q_{N-e} + n_{Cs} Q_{Cs-e} + n_i Q_{ei} \right)^{-1}$$

since  $Q_{ei}$ , given by Eq. (5), is the same for all species. The numerical coefficients of Eqs. (5) and (7) were chosen so that for the extremes of weakly and fully ionized gases, Eq. (7) would assume the forms of the Chapman-Cowling and Spitzer-Härm equations, respectively.

Scalar conductivities (that is, for  $B = 0$ ) of a plasma in thermal equilibrium have been calculated from Eq. (7). The possibility of electrical nonequilibrium was not taken into account. Collision cross sections required in these calculations and the methods used to obtain the particle densities are described in Sections 2.2 and 2.3.

## 2.2 COLLISION CROSS SECTIONS

Much of the uncertainty associated with the calculation of electrical conductivities centers about the validity and availability of collision cross-sectional data. Brown (Ref. 22) and Massey and Burhop (Ref. 23) have collected much of the available cross-sectional data. Brown presents these data in the form of collision probabilities. Also, he has compared experimental cross-sectional data obtained by several investigators in Fig. 1-29 of Ref. 22 to illustrate the chaotic state of experimental disagreement. This is particularly true at low energy levels up to about 1 ev, which is the range of prime interest for the  $\sigma$  calculation described here.

### 2.2.1 Electron-Ion Cross Sections

By virtue of the way that an effective electron-ion collision cross section was found from the Spitzer-Härm equation,  $Q_{ei}$  has been computed for all ion species from Eq. (5).

Typical calculated values of  $Q_{ei}$  are shown in Fig. 1 for argon and argon seeded with 0.1 percent cesium.

### 2.2.2 Electron-Neutral Cross Sections

Since the Chapman and Cowling equation (Eq. (1)) is derived on the basis of the binary diffusion of neutral particles and electrons, cross sections obtained experimentally from diffusion experiments, such as the Townsend method, or calculated diffusion cross sections are required. In the surveys such as Refs. 22 and 23 it is not always clear how the data were obtained. Cross sections obtained from electron beam or Ramsauer-type experiments may be used if an average cross section is computed by the method described in Ref. 8 or 21.

Experimental electron-neutral collision cross sections for argon taken from Refs. 22 through 26 are shown in Fig. 2. All of these data are believed to result from electron diffusion experiments, and the dilemma in selecting appropriate values is apparent. Since the experimental argon cross sections vary widely, two sets of calculations have been made for unseeded argon to demonstrate the magnitude of possible errors because of this uncertainty. The approximate mean values given in Ref. 22 as well as those of Townsend and Bailey (Ref. 25) were used. Lin, Resler, and Kantrowitz (Ref. 8) have also used the latter values and have obtained reasonable agreement with experimental conductivities measured in a shock tube.

In the computation of  $\sigma$  for nitrogen it is necessary to consider both the molecular and atomic species. Comparisons of diffusion cross-sectional data for molecular nitrogen ( $N_2$ ) and atomic nitrogen ( $N$ ) are contained in Fig. 3 (taken from Refs. 22, 23, 27, and 28). Also shown are calculated values of the diffusion cross section which were taken from Refs. 29 through 31. The computed values from Ref. 30 result from Enskog's solution of the Boltzmann equation and were obtained by evaluating the collision integral for a Lennard-Jones potential. Both for  $N_2$  and  $N$  the analytically determined diffusion cross sections compare reasonably well with experiment. Cross sections selected for the present calculations are those given by Massey and Burhop (Ref. 23), but extrapolated at low temperatures as guided by the data of Fisk for  $N_2$  and guided by the Ref. 30 calculations for  $N$ .

Similarly, experimental cross-sectional data available for the alkali metals of interest as seed materials are shown in Fig. 4 (taken from Ref. 32). No other data for Cs, K, or Na could be found in the literature. At the temperatures covered by the calculations here, it was necessary to extrapolate the alkali metal cross-sectional curves to somewhat lower energy levels.

## 2.3 CALCULATION OF NUMBER DENSITY

Number densities of the various species have been obtained by different methods in order to utilize some previous work.

### 2.3.1 Unseeded Argon

Since argon is a monatomic substance its degree of ionization at various temperatures assuming single ionizations was computed from

$$K = \frac{n_e n_i}{n_n} = \frac{\phi^2}{1 - \phi^2} \left( \frac{p_m}{kT} \right) \quad (8)$$

where the degree of ionization,  $\phi$  (that is, the fractional number of ionized particles), is defined as

$$\phi = \frac{n_e}{n_n + n_i} \quad \text{and} \quad n_e = n_i$$

Equilibrium constants for the process  $A \rightarrow A^+ + e^-$  were evaluated by use of the partition functions from

$$K = \left( \frac{2\pi m_e}{h^2} \right)^{3/2} (kT)^{3/2} \frac{Z_e Z_i}{Z_n} \exp \left( \frac{-I_p}{kT} \right) \quad (9)$$

without taking into account the Debye-Hückel lowering of the ionization potential which should be negligible for the range of conditions covered by this study. Values of the equilibrium constants for argon calculated

from Eq. (9), but multiplied by  $kT$ , are shown in Fig. 5. After the computation of  $\phi$  at a given pressure and temperature, the particle densities were found from

$$n_i = n_e = \left( \frac{\phi}{1 + \phi} \right) \frac{p_m}{kT} \quad (10)$$

and

$$n_n = \left( \frac{1 - \phi}{1 + \phi} \right) \frac{p_m}{kT} \quad (11)$$

### 2.3.2 Seeded Argon

At temperatures below about 5000°K it would be sufficiently accurate to consider only the ionization of the seed, but at higher temperatures one must account for the simultaneous ionization of the argon atoms. In the latter and more general case, the derivation of expressions giving the particle densities is straightforward but involves several algebraic manipulations. Appendix I contains this derivation, and only the results are given here.

By use of the Saha equation the degree of seed ionization,  $\phi_s$ , can be obtained from

$$K_s = \frac{\phi_s^2 p_m}{(1 - \phi_s)(C_A + 1 + \phi_s) kT} \quad (12)$$

at temperatures below 7000°K when the degree of argon ionization is slight. For higher temperatures it is sufficiently accurate to take  $\phi_s = 1$ . The seeding rate factor for argon,  $C_A$ , is related to seeding rate,  $S$ , by

$$C_A = \frac{M_s}{M_A} \left( \frac{1 - S}{S} \right) \quad (13)$$

Values of the equilibrium constant,  $K$ , obtained from Eq. (9) for potassium and cesium are also given in Fig. 5. The degree of ionization of the argon,  $\phi_A$ , can next be determined from

$$K_A = \frac{\phi_A^2}{1 - \phi_A} \left\{ \frac{C_A p_m}{kT [1 + \phi_s + C_A (1 + \phi_A)]} \right\} \quad (14)$$

and then the various particle densities expressed in terms of the argon and seed ionization fractions as

$$n_{A_n} = \frac{(1 - \phi_A) C_A p_m}{kT [(1 + \phi_s) + C_A (1 + \phi_A)]} \quad (15)$$



$$n_{s_n} = \frac{(1 - \phi_s) p_m}{kT [(1 + \phi_s) + C_A (1 + \phi_A)]} \quad (16)$$

$$n_{A_i} = \frac{\phi_A C_A p_m}{kT [(1 + \phi_s) + C_A (1 + \phi_A)]} \quad (17)$$

$$n_{s_i} = \frac{\phi_s p_m}{kT [(1 + \phi_s) + C_A (1 + \phi_A)]} \quad (18)$$

$$n_e = \frac{(\phi_s + C_A \phi_A) p_m}{kT [(1 + \phi_s) + C_A (1 + \phi_A)]} \quad (19)$$

### 2.3.3 Unseeded Nitrogen

Particle densities employed in these calculations were supplied by Hilsenrath of the National Bureau of Standards. This work is as yet unpublished, but the calculational procedure basically follows that previously employed by Hilsenrath in his air calculations (Ref. 33). Some of the particle densities used are tabulated in Table 1.

### 2.3.4 Seeded Nitrogen

Calculation of the conductivity of seeded nitrogen also utilized Hilsenrath's nitrogen particle densities. Since the pressure of seeded  $N_2$ ,  $p_m$ , is equal to the sum of the partial pressures of the nitrogen and the seed, the nitrogen particle densities were evaluated at a pressure of

$$p_{N_2} = \left( \frac{C_{N_2}}{C_{N_2} + 1} \right) p_m$$

The equations used to compute the number densities for seeded nitrogen are summarized in Appendix II, but the general procedure was to (1) determine the  $N_2$  plasma number densities at  $p_{N_2}$ ; (2) convert these to mass fractions; (3) add the specified amount of seed and re-evaluate the mass fractions of the new seeded mixture; (4) convert the seeded mixture mass fractions to number densities; and finally, (5) compute the degree of ionization of the seed by use of the Saha equation. The equations are written for the addition of two seed materials in order to treat the case of NaK. For computations with either Cs or K seed alone, the mass of the second seed material was taken as zero.

### 3.0 CALCULATION OF ELECTRICAL CONDUCTIVITY WITH MAGNETIC FIELDS

#### 3.1 TENSOR CONDUCTIVITY EQUATIONS

Since charged particles move under the influence of magnetic fields, the electrical conductivity of an ionized gas in the presence of a magnetic field takes on tensor characteristics. In this case it is convenient to consider the "effective" directional components of the conductivity which may be obtained from a general expression for the current density by arranging it in the standard form of Ohm's law.

With the following assumptions:

- (a) All species are in thermal equilibrium  
( $T_n = T_i = T_e = T_s$ ),
- (b) Only single ionizations occur.
- (c) All forces are in equilibrium but the gravitational force on the electrons and electron acceleration is negligible, and
- (d) Electrons are more free to spiral than ions such that  
( $\omega\tau$ )<sub>en</sub> >> 2( $\omega\tau$ )<sub>in</sub>.

Chapman and Cowling (Ref. 19) have written the equations of motion for (1) electrons, (2) ions, and (3) the gas as a whole. By combining these equations they obtain as the equation of charge motion for a partially ionized gas in the presence of a magnetic field,

$$\begin{aligned} n_e e \vec{E}' + (1 - f\beta) \nabla p_e = (\kappa_{ei} + \beta \kappa_{in}) B \vec{J} + (1 - 2f\beta) \vec{J} \times \vec{B} \\ + \frac{f^2}{B} (\kappa_{en} + \kappa_{in})^{-1} \left[ \nabla p_e \times \vec{B} - (\vec{J} \times \vec{B}) \times \vec{B} \right] \end{aligned} \quad (20)$$

where

$$\kappa_{en} = \frac{1}{\omega_e \tau_{en}}; \quad \kappa_{ei} = \frac{1}{\omega_e \tau_{ei}}; \quad \kappa_{in} = \frac{1}{2\omega_i \tau_{in}} \quad (21)$$

$$\beta = \frac{\kappa_{en}}{\kappa_{en} + \kappa_{in}} \quad (22)$$

$$f = 1 - \phi \quad (23)$$

and

$$\vec{E}' = \vec{E} + \vec{V} \times \vec{B}$$

In Eq. (20),  $\vec{E}'$  and  $\vec{B}$  are the resultant electric and magnetic field vectors, respectively, and in a general sense may have components in all or any of the three rectangular coordinate directions.

Since  $\kappa_{en} \ll \kappa_{in}$ ,  $\beta \ll 1$ , and  $\beta \kappa_{in} \approx \kappa_{en}$ , Brunner (Ref. 1) has simplified Eq. (20) and written it as

$$\begin{aligned} \vec{J}(1 + b) = & \sigma \vec{E}' + \frac{\omega_e \bar{\tau}_e}{B} \nabla p_e - \omega_e \bar{\tau}_e \left( \vec{J} \times \frac{\vec{B}}{B} \right) \\ & - b \left[ \nabla p_e \times \frac{\vec{B}}{B} - \frac{\vec{B}}{B} \left( \frac{\vec{B}}{B} \cdot \vec{J} \right) \right] \end{aligned} \quad (24)$$

where

$$\omega_e \bar{\tau}_e = \omega_e \left( \frac{1}{\tau_{ei}} + \frac{1}{\tau_{en}} \right)^{-1}$$

(often called the Hall parameter)

and

$$b = 2f^2 (\omega_i \tau_{in}) (\omega_e \bar{\tau}_e)$$

(often called the ion-slip factor)

In Eq. (24)  $\sigma$  refers to the scalar conductivity, that is, conductivity with no magnetic field present.

By neglecting the electron pressure gradient and the last term on the right side of Eq. (24), Brunner obtains an expression for the components of current density parallel to  $\vec{E}'$  and in the direction  $\vec{E}' \times \vec{B}$  (that is, direction of the induced Hall field). He then computed the effective conductivity or component of the conductivity in the direction parallel to  $\vec{E}'$  to illustrate the Hall and ion-slip effects induced by a strong magnetic field. His analysis is extended here to allow evaluation of all three main directional components of the conductivity.

If the electron pressure gradient is neglected, Eq. (24) becomes

$$\vec{J}(1 + b) = \sigma \vec{E}' - \omega_e \bar{\tau}_e \left( \vec{J} \times \frac{\vec{B}}{B} \right) + b \frac{\vec{B}}{B} \left( \frac{\vec{B}}{B} \cdot \vec{J} \right) \quad (25)$$

The last term which was neglected by Brunner arises from a term involving  $(\vec{J} \times \vec{B}) \times \vec{B}$  which in a sense may be thought of as the Hall current's, Hall current. Equation (25) may be divided by  $(1 + b)$  and then the vector product  $\vec{J} \times \vec{B}$  taken. If the resulting expression for  $\vec{J} \times \vec{B}$  is substituted

back into Eq. (25), this results in the elimination of the current density from the middle term on the right-hand side of Eq. (25), or

$$\begin{aligned} \vec{J} \left[ (1 + b)^2 + (\omega_e \bar{\tau}_e)^2 \right] &= (1 + b) \sigma \vec{E}' - \sigma (\omega_e \bar{\tau}_e) \vec{E}' \times \frac{\vec{B}}{B} \\ &+ \left[ (\omega_e \bar{\tau}_e)^2 + b(1 + b) \right] \frac{\vec{B}}{B} \left( \frac{\vec{B}}{B} \cdot \vec{J} \right) \end{aligned} \quad (26)$$

Similarly,  $\vec{J}$  can be eliminated from the last term on the right side by taking the scalar product  $\vec{J} \cdot \vec{B}$  of Eq. (26) and substituting it back into Eq. (26). These operations finally allow Eq. (24) to be written in simple ohmic form as

$$\begin{aligned} \vec{J} &= \left[ \frac{(1 + b)}{(\omega_e \bar{\tau}_e)^2 + (1 + b)^2} \right] \sigma \vec{E}' - \left[ \frac{\omega_e \bar{\tau}_e}{(\omega_e \bar{\tau}_e)^2 + (1 + b)^2} \right] \sigma \left( \vec{E}' \times \frac{\vec{B}}{B} \right) \\ &+ \left[ \frac{(\omega_e \bar{\tau}_e)^2 + b(1 + b)}{(\omega_e \bar{\tau}_e)^2 + (1 + b)^2} \right] \sigma \left[ \frac{\vec{B}}{B} \left( \vec{E}' \cdot \frac{\vec{B}}{B} \right) \right] \end{aligned} \quad (27)$$

Equation (27) then gives the components of the current density and conductivity in the three directions given by the vector terms. The term  $\sigma$  represents the scalar conductivity as might be computed from the methods given in the previous section, and the three components of the conductivity are

1. Parallel to the resultant  $\vec{E}'$ -field

$$\sigma_{\text{eff}} = \left[ \frac{1 + b}{(\omega_e \bar{\tau}_e)^2 + (1 + b)^2} \right] \sigma \quad (28)$$

2. Perpendicular to both  $\vec{E}'$  and  $\vec{B}$

$$\sigma_{\text{eff}} = \left[ \frac{\omega_e \bar{\tau}_e}{(\omega_e \bar{\tau}_e)^2 + (1 + b)^2} \right] \sigma \quad (29)$$

3. Parallel to the resultant  $\vec{B}$ -field

$$\sigma_{\text{eff}} = \left[ \frac{(\omega_e \bar{\tau}_e)^2 + b(1 + b)}{(\omega_e \bar{\tau}_e)^2 + (1 + b)^2} \right] \sigma \quad (30)$$

An interpretation of these component equations in terms of the effective conductivity which would exist in various types of MHD power generators or accelerators is given later.

These results can be derived in a more elegant manner by writing Eq. (25) in matrix form as

$$(1 + b) \begin{vmatrix} J_x \\ J_y \\ J_z \end{vmatrix} + \frac{\omega_e \bar{\tau}_e}{B} \begin{vmatrix} J_y B_z - J_z B_y \\ J_z B_x - J_x B_z \\ J_x B_y - J_y B_x \end{vmatrix} - b \left[ \frac{J_x B_x + J_y B_y + J_z B_z}{B^2} \right] \begin{vmatrix} B_x \\ B_y \\ B_z \end{vmatrix} = \sigma \begin{vmatrix} E'_x \\ E'_y \\ E'_z \end{vmatrix} \quad (31)$$

By performing the indicated matrix additions and subtractions, Eq. (31) can be put in the form

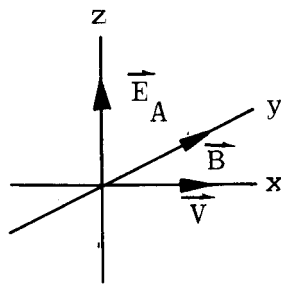
$$\begin{vmatrix} a_{11} & a_{12} & a_{13} \\ a_{21} & a_{22} & a_{23} \\ a_{31} & a_{32} & a_{33} \end{vmatrix} \begin{vmatrix} J_x \\ J_y \\ J_z \end{vmatrix} = \sigma \begin{vmatrix} E'_x \\ E'_y \\ E'_z \end{vmatrix} \quad (32)$$

and by inversion of the matrix  $\alpha$ , Eq. (32) can be arranged in the standard ohmic form

$$\begin{vmatrix} J_x \\ J_y \\ J_z \end{vmatrix} = \sigma \begin{vmatrix} \beta_{11} & \beta_{12} & \beta_{13} \\ \beta_{21} & \beta_{22} & \beta_{23} \\ \beta_{31} & \beta_{32} & \beta_{33} \end{vmatrix} \begin{vmatrix} E'_x \\ E'_y \\ E'_z \end{vmatrix} \quad (33)$$

The various terms for both square matrices are contained in Appendix III, Eqs. (III-3) and (III-4). With the matrix terms from Appendix III, Eq. (27) may be obtained then from Eq. (33).

Effective conductivities in practical MHD channels can be easily obtained from Eqs. (III-3) and (III-4) in Appendix III. Three of the most



important cases are given below and illustrate the application of tensor conductivity. In each case one-dimensional flow is considered with the orientation shown in the adjacent sketch. Moreover, induced magnetic fields will be neglected; that is, low magnetic Reynolds number is assumed.

### 3.1.1 Case A - Segmented Electrodes

When the electrodes are segmented, each electrode pair can assume a different base potential level determined by the Hall voltage. In this

case a Hall potential exists, but there is no Hall current flow. Then,

$$\begin{aligned} B_x &= 0 & E_x &= E_H & J_x &= 0 \\ B_y &= B & E_y &= 0 & J_y &= 0 \\ B_z &= 0 & E_z &= E_A & J_z &= J \end{aligned}$$

With these components, Eqs. (III-3) and (III-4) reduce to

$$\begin{aligned} J_x &= 0 = (1 + b) E_H + \omega_e \bar{\tau}_e E_A \\ J_y &= 0 \\ J_z &= J = \frac{(1 + b) \sigma E_A}{(1 + b)^2 + (\omega_e \bar{\tau}_e)^2} - \frac{\omega_e \bar{\tau}_e \sigma E_H}{(1 + b)^2 + (\omega_e \bar{\tau}_e)^2} \end{aligned}$$

or

$$J = \frac{\sigma}{(1 + b)} E_A$$

Thus, for segmented electrode channels the scalar conductivity is reduced by the factor  $(1 + b)$ , and the reduction only depends upon ion slip.

### 3.1.2 Case B – Continuous Electrodes

With infinite continuous electrodes, the Hall potential would be shorted out, and there would be a maximum axial Hall current such that

$$\begin{aligned} B_x &= 0 & E_x &= 0 & J_x &= J_H \\ B_y &= B & E_y &= 0 & J_y &= 0 \\ B_z &= 0 & E_z &= E & J_z &= J_A \end{aligned}$$

Using Eqs. (III-3) and (III-4), the current components in the x, y, and z directions are found to be

$$J_x = J_H = \frac{(\omega_e \bar{\tau}_e) E_A \sigma}{(1 + b)^2 + (\omega_e \bar{\tau}_e)^2}$$

$$J_y = 0$$

$$J_z = J_A = \frac{(1 + b) \sigma E_A}{(1 + b)^2 + (\omega_e \bar{\tau}_e)^2}$$

In this case the effective electrical conductivity transverse the plasma is given by Eq. (28) since the electric field is in that direction, whereas for the Hall current flow the effective conductivity is given by Eq. (29).

### 3.1.3 Case C – Hall Generator or Accelerator

In this case the components are

$$B_x = 0 \quad E_x = E_H \quad J_x = J_H$$

$$B_y = B \quad E_y = 0 \quad J_y = 0$$

$$B_z = 0 \quad E_z = VB \quad J_z = J_i$$

and expansion of the matrix in Eqs. (III-3) and (III-4) yields

$$J_x = J_H = \frac{(1 + b) \sigma E_H}{(1 + b)^2 + (\omega_e \bar{\tau}_e)^2} + \frac{\omega_e \bar{\tau}_e (VB) \sigma}{(1 + b)^2 + (\omega_e \bar{\tau}_e)^2}$$

$$J_y = 0$$

$$J_z = J_i = \frac{-(\omega_e \bar{\tau}_e) \sigma E_H}{(1 + b)^2 + (\omega_e \bar{\tau}_e)^2} + \frac{(1 + b) (VB) \sigma}{(1 + b)^2 + (\omega_e \bar{\tau}_e)^2}$$

The effective conductivities for Hall devices are given also by Eqs. (28) and (29).

Equation (27) may be simplified to the case of a fully ionized gas by taking  $\phi = 1$  and hence  $b = 0$ ; in which case the conductivity components become:

1. Parallel to the effective  $\vec{E}'$ -field

$$\sigma_{eff_f} = \left[ \frac{1}{(\omega_e \bar{\tau}_e)^2 + 1} \right] \sigma \quad (34)$$

2. Perpendicular to both  $\vec{E}'$  and  $\vec{B}$

$$\sigma_{eff_f} = \left[ \frac{(\omega_e \bar{\tau}_e)}{(\omega_e \bar{\tau}_e)^2 + 1} \right] \sigma \quad (35)$$

3. Parallel to the  $\vec{B}$ -field

$$\sigma_{eff_f} = \left[ \frac{(\omega_e \bar{\tau}_e)^2}{(\omega_e \bar{\tau}_e)^2 + 1} \right] \sigma \quad (36)$$

### 3.2 ION-NEUTRAL CROSS SECTIONS

The mean free time between collisions is related to the collision cross section by

$$\tau = \frac{1}{\bar{v} n Q}$$

or specifically,

$$\tau_{in} = \sqrt{\frac{\pi m_i}{8kT}} \frac{1}{n_n Q_{in}} \quad (37)$$

$$\tau_{ei} = \sqrt{\frac{\pi m_e}{8kT}} \frac{1}{n_e Q_{ei}} \quad (38)$$

$$\tau_{en} = \sqrt{\frac{\pi m_e}{8kT}} \frac{1}{n_n Q_{en}} \quad (39)$$

when the particles have a Maxwellian distribution.

Determination of all of the terms in Eqs. (37) through (39) except  $Q_{in}$  is discussed in Sections 2.2 and 2.3. However, values of the ion-neutral collision cross sections must now also be specified.

Some collision cross-sectional data for cesium and potassium ions in argon are shown in Fig. 6a and for potassium ions in molecular nitrogen in Fig. 6b. These data taken from Ref. 22 were obtained at high energy levels and require an extensive extrapolation to the range of interest here. Because the cesium-in-argon curve becomes very steep with decreasing energy level, an extrapolation was felt to be too impractical. However; extrapolations guided by other existing data for different substances have made for the other two curves. The validity of these gross extrapolations is certainly subject to doubt. Unfortunately, no existing data could be found for collisions between potassium ions and atomic nitrogen neutrals, and consequently, subsequent calculations of the effective electrical conductivity in the primary directions for fully ionized gases would be expected to be less accurate than those for partially ionized gases.

## 4.0 NUMERICAL COMPUTATIONS

### 4.1 SCALAR CONDUCTIVITY

#### 4.1.1 Argon

Scalar electrical conductivities of unseeded argon at pressures of 0.01, 0.1, 1.0, and 10 atm were computed by use of Eq. (7) by using the electron-neutral collision cross sections obtained by Townsend and Bailey (Ref. 25) (shown herein by the dashed curve in Fig. 2). Additional



calculations have been made for unseeded argon at pressures from  $10^{-2}$  to  $10^3$  atm using the electron-neutral argon cross sections contained in Ref. 22 and shown in Fig. 2 by the dash-dot curve in order to make an estimate of the possible errors introduced by lack of exact knowledge of the cross section. Results of these conductivity calculations are given in Figs. 7a and b, respectively, and are shown to agree within about 50 to 75 percent.

Calculated values of the conductivity of argon seeded with cesium are given in Fig. 8, whereas Fig. 9 gives the results for potassium-seeded argon. For the seeded case only the Townsend-Bailey cross sections are used to represent the electron-argon collisions. Pressure varying from  $10^{-2}$  to 10 atm is used as a parameter for these conductivity curves to demonstrate its effect at seeding rates of 0.01, 0.1, 1.0, and 10 percent seed weight to the total weight.

#### 4.1.2 Nitrogen

Calculated scalar conductivities for unseeded nitrogen at pressure levels from 0.01 to 10 atm are shown in Fig. 10. In this case the electron-neutral cross sections used are those taken from Ref. 23 and shown here in Fig. 3. In addition, conductivities of nitrogen seeded with either cesium, potassium, or NaK in the amounts of 0.01, 0.10, 0.3, 0.7, 1.0, and 10.0 percent seed by weight are presented in Figs. 11 through 13, respectively. In these figures, seeding rate is used as a parameter instead of pressure to demonstrate its effect on the conductivity. Calculations were made for NaK consisting of 78 percent potassium by weight.

The initial increase in the conductivity with temperature is caused by ionization of the seed material. As the temperature increases, the conductivity reaches an intermediate peak value where nearly all of the seed is ionized. With further increase in temperature the conductivity begins to diminish. This occurs because the curve was calculated for a constant pressure; thus the particle density and hence electron density decreases with increasing temperature faster than electrons are created by  $N_2$  ionization. The conductivity begins to increase again when the temperature is high enough that a significant number of electrons are liberated in the  $N_2$ . Conductivities for a given seeding rate tend to merge into those for the unseeded case. As the nitrogen ionization approaches completeness, there is little effect of seed addition; however, at temperatures below 6000°K seeding can increase the conductivity several orders of magnitude.

## 4.2 TENSOR CONDUCTIVITY

Typical values of the Hall parameter ( $\omega_e \bar{\tau}_e$ ) and the ion-slip factor (b) are given in Figs. 14 and 15, respectively, since their magnitude indicates the importance of tensor conductivity effects. They have been divided by B and  $B^2$  so that they may be scaled to any level of the magnetic field; the actual values shown correspond to  $B = 1$  weber/m<sup>2</sup> (10,000 gauss).

Figure 15 indicates that the effective conductivity in a MHD channel with segmented electrodes would be less than one percent lower than the scalar conductivity at atmospheric pressure and for seed rates between 0.1 and 1 percent (by weight) when the magnetic field is 10,000 gauss. The scalar conductivity would be reduced by about 2 percent if the B-field is increased to 20,000 gauss. At lower pressures where ion slip becomes much more important, however, there will be a significant reduction of the scalar conductivity when a strong magnetic field is applied.

To further illustrate the importance of tensor conductivity the three basic tensor components which could result when magnetic fields are applied to the plasma have been calculated by evaluating  $\sigma_{\text{eff}}/\sigma$  from Eqs. (28) through (30). These calculations have primarily been made in the weakly ionized range ( $1000^\circ\text{K} \leq T \leq 4000^\circ\text{K}$ ), but the fully ionized limit, given by Eqs. (34) through (36), was also computed (assuming  $T = 15,000^\circ\text{K}$  for the evaluation of  $\omega_e \bar{\tau}_e$  and b). Effects of the magnetic field on the conductivity of nitrogen at atmospheric pressure and seeded with 0.1 percent potassium are shown in Fig. 16. It is apparent that the effective conductivity in the direction of the effective electric field decreases rapidly with increasing magnetic field strength. A similar comparison is made in Fig. 17 for a 1 percent seed rate. Influence of seeding rate may be observed by comparison of Figs. 16 and 17 and effects of pressure by comparison of Figs. 16a and b or 17a and b.

The reduction of scalar conductivity which might be expected in channels with continuous electrodes or Hall devices is indicated by these figures.

## 4.3 VALIDITY OF CALCULATIONS

The accuracy of the computed conductivities depends of course upon the reliability of the cross sections used. Various experimental values of the electron-neutral cross sections available in the literature have already been presented and, at least for the case of unseeded argon, the magnitude of possible errors introduced by the electron-neutral term has been estimated. In any event, if more accurate cross sections

become available in the future, the present calculations could be updated. Additionally, the definition of the electron-ion cross section as employed here also raises some questions.

Spitzer points out in Ref. 34 that his theory breaks down for values of  $\ln \Lambda$  less than about five, that is, at low temperatures and/or high pressures. There has been some experimental agreement with the Spitzer-Härm theory (Eq. (2)) from several sources (for example Ref. 8) for values of  $\ln \Lambda$  between three and six. However, Spitzer, himself, states that this agreement is only fortuitous. For many of the calculations presented here,  $\ln \Lambda$  falls in this dubious range. Because of the way the conductivity equation has been arranged, the doubt arises in the definition of  $Q_{ei}$  in Eq. (5). It may be that the calculated effective electron-ion collision cross section is greater than the actual value. Since the estimated values of  $Q_{ei}$  are from  $10^3$  to  $10^4$  times the typical values for the electron-neutral cross section, the computed conductivity is dominated by  $Q_{ei}$  over a wider range than may actually occur. This is particularly true for seeded gases where an appreciable electron number density exists at low temperatures. A careful experimental study of the conductivity of seeded gas offers the possibility of defining the range over which the Spitzer-Härm equation is valid and still experiment with gases at reasonable temperatures. In any event, one might question the calculations presented here when  $\ln \Lambda$  falls below 4.5 to 5.0, and, if possible, the calculated results should be checked by experiment. Table 2 contains typical values of  $\ln \Lambda$  for the present calculations. Calculated conductivities of gases at higher pressure are certainly doubtful; for example, the calculation for argon at  $p = 10^2$  to  $10^3$  atm presented herein should be viewed critically.

In the lower temperature range where Eq. (7) is dominated by  $Q_{en}$  terms the calculated results are believed to be reliable, since the Chapman-Cowling equation has been checked by several sources of experimental data.

## REFERENCES

1. Brunner, M. J. "The Effects of Hall and Ion Slip on the Electrical Conductivity of Partially Ionized Gases for Magnetohydrodynamic Re-entry Vehicle Application." ASME Paper 61-WA-176, January 1962.
2. Frost, L. S. "Conductivity of Seeded Atmospheric Pressure Plasma." Journal of Applied Physics, Vol. 32, No. 10, October 1961.
3. Arave, R. J. and Huseby, O. A. "Aerothermodynamic Properties of High Temperature Argon." Boeing Report No. D2-11238, October 1962.

4. Friel, P. J. "Electron Density and Electrical Conductivity of High Temperature Air Seeded with the Alkali and Alkaline Earth Metals." Missile and Space Vehicle Department, General Electric, Technical Information Series Report No. R59SD459, December 1959.
5. Chinitz, W., et al. "Aerothermodynamic Properties of Some Gas Mixtures to Mach 20." American Rocket Society Journal, Vol. 29, No. 8, August 1959, p. 573.
6. Way, S., et al. "Long Life Closed Loop MHD Research and Development Unit." Westinghouse Research Laboratories, Pittsburgh, Penn., AD 284753, September 1962.
7. Mullaney, G. J., et al. "Electrical Conductivity in Flame Gases with Large Concentration of Potassium." Journal of Applied Physics, Vol. 32, No. 4, April 1961, p. 668.
8. Lin, Shao-Chi, Resler, E. L., and Kantrowitz, A. "Electrical Conductivity of Highly Ionized Argon Produced by Shock Waves." Journal of Applied Physics, Vol. 26, No. 1, January 1955, p. 95.
9. Smy, P. R. and Driver, H. S. "Electrical Conductivity of Low-Pressure Shock-Ionized Argon." Journal of Fluid Mechanics, Vol. 17, Part 2, October 1963, p. 182.
10. Harris L. P. "Electrical Conductivity of Cesium-Seeded Atmospheric Pressure Plasma near Thermal Equilibrium." Journal of Applied Physics, Vol. 34, No. 10, October 1963, p. 2958.
11. Lapp, M. and Rich, J. A. "Electrical Conductivity of Seeded Flame Plasmas in Strong Electric Fields." The Physics of Fluids, Vol. 6, No. 6, June 1963, p. 806.
12. Anon. M. P. D. Electrical Power Generation. Published by The Institute of Electrical Engineers, Savoy Place, London, September 1962. See Section entitled Seeded Combustion Plasmas, pp. 90-106.
13. Moore, George E. "Experimental Studies of Some Electrical Properties of Seeded Flame Gases." ARS Ions in Flames and Rocket Exhausts Conference, October 10-12, 1962.
14. Dimmock, T. H., et al. "Electrical Properties of Rocket Flames." ARS Ions in Flames and Rocket Exhausts Conference, October 10-12, 1962.
15. Lamb, L. and Lin, S. C. "Electrical Conductivity of Thermally Ionized Air Produced in a Shock Tube." Journal of Applied Physics, Vol. 28, No. 7, July 1957, p. 754.

16. Sonnerup, B. "Some Effects of Tensor Conductivity in Magneto-hydrodynamics." Journal of the Aerospace Sciences, Vol. 28, No. 8, August 1961.
17. Kerrebrock, J. L. "Conduction in Gases with Elevated Electron Temperature." Second Symposium on Engineering Aspects of Magnetohydrodynamics, March 9-10, 1961.
18. Kerrebrock, J. L. and Hoffman, M. A. "Experiments on Non-equilibrium Ionization Due to Electron Heating." AIAA Aerospace Sciences Meeting, New York, January 19-22, 1964, Preprint No. 64-27.
19. Chapman, S. and Cowling, T. G. The Mathematical Theory of Non-Uniform Gases. Cambridge University Press, Cambridge, England, 1939.
20. Spitzer, L., Jr. and Härm, R. "Transport Phenomena in a Completely Ionized Gas." Physical Review, Vol. 89, 1953, p. 997.
21. Sherman A. "Calculation of Electrical Conductivity of Ionized Gases." American Rocket Society Journal, Vol. 30, No. 8, June 1960.
22. Brown, S. C. Basic Data of Plasma Physics. The Technology Press, Massachusetts Institute of Technology, and John Wiley and Sons, Inc., New York, 1959.
23. Massey, H. S. W. and Burhop, E. H. S. Electronic and Ionic Impact Phenomena. Oxford University Press, London, 1952.
24. Bond, J. W., Jr. "The Structure of a Shock Front in Argon." Los Alamos Scientific Laboratory of the University of California, LA-1693, July 1954.
25. Townsend, J. S. and Bailey, V. A. Philosophical Magazine, Vol. 43, 1922, p. 593, and Vol. 44, 1922, p. 1033.
26. Wahlin, H. B. Physical Review. Vol. 37, 1931, p. 260.
27. Fisk, J. B. Physical Review. Vol. 49, 1936, p. 167.
28. Shkarofsky, I. P., Bachynski, M. P., and Johnson, T. W. "Collision Frequency Associated with High Temperature Air and Scattering Cross Sections of the Constituents." RCA, Research Report No. 7-8015, March 1960.
29. Prasad, S. S. and Prasad, K. "Classical Calculations for Impact Ionization Cross Sections." Proceedings of the Physical Society, Vol. 82, Part 5, November 1963, p. 655.

30. Peng, T. C. and Pindroh, A. L. "An Improved Calculation of Gas Properties at High Temperatures - Air." Boeing Report D2-11722, February 1962.
31. Robinson, L. B. "Elastic Scattering of Low-Energy Electrons by Atomic Nitrogen and Atomic Oxygen." Physical Review, Vol. 105, No. 3, February 1957.
32. Brode, R. B. "The Quantitative Study of the Collision of Electrons with Atoms." Reviews of Modern Physics, Vol. 5, October 1933, p. 257.
33. Hilsenrath, J. and Klein, M. "Tables of Thermodynamic Properties of Air in Chemical Equilibrium Including Second Virial Corrections from 1500°K to 15,000°K." AEDC-TDR-63-161 (AD 416040), August 1963.
34. Spitzer, Lyman, Jr. Physics of Fully Ionized Gases. Interscience Publishers, Division of John Wiley and Sons, New York, 1962. (Second Edition, No. 3)

## APPENDIX I

## CALCULATION OF PARTICLE DENSITIES FOR SEEDED ARGON

The mixture pressure of seeded argon is the sum of the partial pressures of all of the species. If each specie is represented by the perfect gas law and the mixture is in thermal equilibrium,

$$p_m = \sum n_j kT = (n_{A_n} + n_{A_i} + n_{A_e} + n_{s_n} + n_{s_i} + n_{s_e})kT \quad (I-1)$$

The following definitions are made:

$$\phi_A = \frac{n_{A_e}}{n_{A_n} + n_{A_i}} \quad (I-2)$$

$$\phi_s = \frac{n_{s_e}}{n_{s_n} + n_{s_i}} \quad (I-3)$$

$$\frac{n_A}{n_s} = C_A = \frac{M_s}{M_A} \left( \frac{1-S}{S} \right) \quad (I-4)$$

where  $n_A$  and  $n_s$  represent the number densities at normal conditions, that is, before ionization becomes significant, while the various  $n_j$ 's ( $n_{A_n}$ ,  $n_{A_i}$ , . . . . .  $n_{s_e}$ ) are the number densities of the various species after ionization. Further, it is assumed that only single ionizations occur so that  $n_{s_i} = n_{s_e}$  and  $n_{A_i} = n_{A_e}$ .

Making use of the Saha equation

$$K_s = \frac{n_{s_e} n_{s_i}}{n_{s_n}} = \left( \frac{2\pi m_e}{h^2} \right)^{3/2} (kT)^{3/2} \frac{Z_e Z_i}{Z_n} \exp \left( \frac{-I_{p_s}}{kT} \right) \quad (I-5)$$

the equilibrium constant may be determined from the right side of the equation.

Substitution of Eqs. (I-1) and (I-3) into (I-5) results in

$$K_s = \frac{\phi_s^2 p_m}{(1 - \phi_s) \left( 1 + \phi_s + \frac{n_{A_n} + n_{A_i} + n_{A_e}}{n_{s_i} + n_{s_n}} \right) kT}$$

Then Eqs. (I-2) and (I-4) may be used to eliminate the remaining number density terms, so that

$$K_s = \frac{\phi_s^2 p_m}{(1 - \phi_s) [1 + \phi_s + C_A (1 + \phi_A)] kT} \quad (I-6)$$

In a similar manner, one can arrive at an equation from which the degree of ionization of argon may be obtained,

$$K_A = \frac{C_A \phi_A^2 p_m}{(1 - \phi_A) [1 + \phi_s + C_A (1 + \phi_A)] kT} \quad (I-7)$$

Note that Eqs. (I-6) and (I-7) are coupled. In principle, the ionization of the seed and argon atoms occurs simultaneously, and thus these two equations must be solved simultaneously. Fortunately, from a practical standpoint it is not necessary to do this since the seed usually becomes fully ionized before the argon begins to ionize in any appreciable amount. For the range of the calculations considered here it is sufficiently accurate to neglect the  $C_A \phi_A$  term in computations of  $\phi_s$  from Eq. (I-6) for temperatures below 7000°K since  $C_A \phi_A \ll C_A$ , whereas at higher temperatures the seed ionization is nearly complete and a value of  $\phi_s = 1$  may be used.

With the degree of ionization for both the seed and the argon determined from Eqs. (I-6) and (I-7), the individual specie number densities may be determined by manipulations of Eq. (I-1). For example, one can easily show that

$$(1 + \phi_s) + C_A (1 + \phi_A) = \frac{n_{s_n} + n_{s_i} + n_{s_e} + n_{A_n} + n_{A_i} + n_{A_e}}{n_{s_n} + n_{s_i}}$$

Then, using Eq. (I-1)

$$\frac{p_m}{kT [(1 + \phi_s) + C_A (1 + \phi_A)] (n_{s_n} + n_{s_i})} = 1$$

and multiplying by  $n_{s_n}$  gives

$$n_{s_n} = \frac{(1 - \phi_s) p_m}{kT [(1 + \phi_s) + C_A (1 + \phi_A)]} \quad (I-8)$$

since

$$\frac{n_{s_n}}{n_{s_n} + n_{s_i}} = 1 - \phi_s \quad \text{and} \quad n_{s_i} = n_{s_e}$$



Similarly, the other particle densities may be shown to be

$$n_{s_i} = \frac{\phi_s P_m}{kT [(1 + \phi_s) + C_A (1 + \phi_A)]} \quad (\text{I-9})$$

$$n_{A_n} = \frac{(1 - \phi_A) C_A P_m}{kT [(1 + \phi_s) + C_A (1 + \phi_A)]} \quad (\text{I-10})$$

$$n_{A_i} = \frac{\phi_A C_A P_m}{kT [(1 + \phi_s) + C_A (1 + \phi_A)]} \quad (\text{I-11})$$

and

$$n_e = n_{A_i} + n_{s_i} = \frac{(\phi_A C_A + \phi_s) P_m}{kT [(1 + \phi_s) + C_A (1 + \phi_A)]} \quad (\text{I-12})$$

## APPENDIX II

## CALCULATION OF PARTICLE DENSITIES FOR SEEDED NITROGEN

Equilibrium particle densities for pure nitrogen which have been calculated by Hilsenrath are employed for all  $N_2$  calculations. A few of these particle densities are given in Table 1. When the seed is added to the  $N_2$ , the new mixture pressure is

$$P_m = P_g + P_s$$

It is desired to calculate the conductivity at a specified value of  $p_m$ , but the nitrogen particle densities should be selected at the  $N_2$  partial pressure  $p_g$ . For perfect gases in equilibrium

$$C = \frac{n_g}{n_s} = \frac{p_g}{p_s}$$

Thus,

$$p_g = \left( \frac{C}{C + 1} \right) p_m \quad (\text{II-1})$$

At pressures given by Eq. (II-1) and a specified temperature, the number densities or mole fractions of  $N_2$  were found from tables such as Table 1 and converted to specie mass fractions ( $Y_j$ ) by

$$Y_j = (X_j)(M_j) / \sum X_j M_j$$

Then, the mass of seed as specified by  $S$  is added to the mixture and the new specie mass fractions evaluated from

$$Y'_{N_2} = \frac{X_{N_2} M_{N_2}}{\sum X_j M_j} (1 - S)$$

$$\begin{matrix} \cdot & \cdot \\ \cdot & \cdot \\ \cdot & \cdot \end{matrix}$$

$$Y'_{N_i} = \frac{X_{N_i} M_{N_i}}{\sum X_j M_j} (1 - S)$$

$$Y'_s = S$$

Primed quantities denote the new mixture. These in turn are converted to molar fractions or number fractions for the new mixture;

$$\begin{aligned}
 X'_{N_2} &= \frac{(1-S) \frac{X_{N_2}}{\sum X_j M_j}}{\frac{1-S}{\sum X_j M_j} + \frac{S}{M_s}} \\
 &\vdots \\
 X'_{N_i} &= \frac{(1-S) \frac{X_{N_i}}{\sum X_j M_j}}{\frac{1-S}{\sum X_j M_j} + \frac{S}{M_s}} \\
 X'_s &= \frac{\frac{S}{M_s}}{\frac{1-S}{\sum X_j M_j} + \frac{S}{M_s}}
 \end{aligned}$$

Since each specie is assumed to be perfect gas, the total number of particles present may be determined from

$$n'_T = \frac{p_m N_o}{RT}$$

If two seed materials are used, let A represent the mass fraction of one seed with respect to the total amount of seed. Further, if the seeds do not react with each other or with the N<sub>2</sub> plasma species, their original number densities may be similarly computed from

$$n_{s_1} = \frac{(A)(S) N_o p_m M_m}{M_{s_1} RT}$$

and

$$n_{s_2} = \frac{(1-A) S N_o p_m M_m}{M_{s_2} RT}$$

where the new mixture molecular weight is given by

$$M_m = (X'_{N_2} + X'_{N_{2i}})(28.016) + (X'_N + X'_{N_i})(14.008) + X'_{s_1} M_{s_1} + X'_{s_2} M_{s_2}$$

Then the degree of ionization for each seed material may be computed from

$$K_{s_1}(kT) = \frac{\phi_{s_1}^2}{(1-\phi_{s_1})} n_{s_1}(kT)$$

and

$$K_{s_2}(kT) = \frac{\phi_{s_2}^2}{(1 - \phi_{s_2})} n_{s_2}(kT)$$

Finally, from several of the above expressions the number densities of each individual specie may be evaluated from

$$n'_{N_2} = X'_{N_2} n'_T$$

$$\begin{matrix} \cdot \\ \cdot \\ \cdot \\ \cdot \end{matrix}$$

$$n'_{N_i} = X'_{N_i} n'_T$$

$$n'_{s_{1i}} = \phi_{s_1} n'_{s_1}$$

$$n'_{s_{1n}} = (1 - \phi_{s_1}) n'_{s_1}$$

$$n'_{s_{2i}} = \phi_{s_2} n'_{s_2}$$

$$n'_{s_{2n}} = (1 - \phi_{s_2}) n'_{s_2}$$

$$n'_e = n'_{N_{2i}} + n'_{N_i} + n'_{s_{1i}} + n'_{s_{2i}}$$

## APPENDIX III

## TENSOR CONDUCTIVITY EQUATIONS

Writing Eq. (25) in matrix form results in

$$(1 + b) \begin{vmatrix} J_x \\ J_y \\ J_z \end{vmatrix} + \frac{\omega_e \bar{\tau}_e}{B} \begin{vmatrix} J_y B_z - J_z B_y \\ J_z B_x - J_x B_z \\ J_x B_y - J_y B_x \end{vmatrix} - \frac{b(J_x B_x + J_y B_y + J_z B_z)}{B^2} \begin{vmatrix} B_x \\ B_y \\ B_z \end{vmatrix} = \sigma \begin{vmatrix} E_x' \\ E_y' \\ E_z' \end{vmatrix} \quad (\text{III-1})$$

where  $\sigma$  is the scalar conductivity.

If the indicated matrix additions and subtractions are performed the resulting equation may be put in the form of

$$\begin{bmatrix} 1 + b - \frac{b B_x^2}{B^2} & \left[ \frac{\omega_e \bar{\tau}_e B_z}{B} - \frac{b B_x B_y}{B^2} \right] & \left[ - \left( \frac{\omega_e \bar{\tau}_e B_y}{B} + \frac{b B_x B_z}{B^2} \right) \right] \\ - \left( \frac{\omega_e \bar{\tau}_e B_z}{B} + \frac{b B_x B_y}{B^2} \right) & 1 + b - \frac{b B_y^2}{B^2} & \left[ \frac{\omega_e \bar{\tau}_e B_x}{B} - \frac{b B_y B_z}{B^2} \right] \\ \left[ \frac{\omega_e \bar{\tau}_e B_y}{B} - \frac{b B_x B_z}{B^2} \right] & \left[ - \left( \frac{\omega_e \bar{\tau}_e B_x}{B} + \frac{b B_y B_z}{B^2} \right) \right] & 1 + b - \frac{b B_z^2}{B^2} \end{bmatrix} \begin{vmatrix} J_x \\ J_y \\ J_z \end{vmatrix} = \sigma \begin{vmatrix} E_x' \\ E_y' \\ E_z' \end{vmatrix} \quad (\text{III-2})$$

The terms in the square matrix are given as  $\alpha_{11}$  to  $\alpha_{33}$  in Eq. (32) of Section 3.1.

Equation (III-2) may be put in the usual form of Ohm's law by inversion of the first 3 by 3 matrix term. The inversion is a lengthy algebraic process; consequently only the main features are given here. If Eq. (III-2) is expressed

$$|A| |J| = \sigma |E'|$$

then by inverting  $|A|$  it becomes

$$|J| = \sigma |A|^{-1} |E'| = \sigma \frac{\text{adj } |A|}{\det |A|} |E'|$$

The determinant of A,  $\det |A|$ , is found in the usual way and after several manipulations is simplified to

$$\det |A| = (1 + b)^2 + (\omega_e \bar{\tau}_e)^2$$

The adjoint of A,  $\text{adj } |A|$ , is evaluated term by term and results finally in

$$\text{adj } |A| = \begin{vmatrix} \left[ \frac{B_x^2}{B^2} [(\omega_e \bar{\tau}_e)^2 + b(1 + b)] + (1 + b) \right] \left[ \frac{B_x B_y}{B^2} [(\omega_e \bar{\tau}_e)^2 + b(1 + b)] - \frac{\omega_e \bar{\tau}_e}{B} B_z \right] \left[ \frac{B_x B_z}{B^2} [(\omega_e \bar{\tau}_e)^2 + b(1 + b)] + \frac{\omega_e \bar{\tau}_e}{B} B_y \right] \\ \left[ \frac{B_x B_y}{B^2} [(\omega_e \bar{\tau}_e)^2 + b(1 + b)] + \frac{\omega_e \bar{\tau}_e}{B} B_z \right] \left[ \frac{B_y^2}{B^2} [(\omega_e \bar{\tau}_e)^2 + b(1 + b)] + (1 + b) \right] \left[ \frac{B_y B_z}{B^2} [(\omega_e \bar{\tau}_e)^2 + b(1 + b)] - \frac{\omega_e \bar{\tau}_e}{B} B_x \right] \\ \left[ \frac{B_x B_z}{B^2} [(\omega_e \bar{\tau}_e)^2 + b(1 + b)] - \frac{\omega_e \bar{\tau}_e}{B} B_y \right] \left[ \frac{B_y B_z}{B^2} [(\omega_e \bar{\tau}_e)^2 + b(1 + b)] + \frac{\omega_e \bar{\tau}_e}{B} B_x \right] \left[ \frac{B_z^2}{B^2} [(\omega_e \bar{\tau}_e)^2 + b(1 + b)] + (1 + b) \right] \end{vmatrix} \quad (\text{III-3})$$

The terms of this matrix divided by the  $\det |A|$  are listed as  $\beta_{11}$  through  $\beta_{33}$  in Eq. (33). In its final matrix form the current density may be

$$\begin{vmatrix} J_x \\ J_y \\ J_z \end{vmatrix} = \frac{\sigma}{[(1 + b)^2 + (\omega_e \bar{\tau}_e)^2]} \text{adj } |A| \begin{vmatrix} E'_x \\ E'_y \\ E'_z \end{vmatrix} \quad (\text{III-4})$$

where Eq. (III-3) gives  $\text{adj } |A|$ . Various components of the tensor conductivity in the most general case are given by Eqs. (III-3) and (III-4).

For the case of orthogonal fields and the gas fully ionized, Eq. (III-4) takes on a much simpler form. Taking the fields mutually perpendicular with the following directions,

$$\begin{aligned}\vec{E} &= \vec{j} E \\ \vec{B} &= \vec{k} B \\ \vec{V} &= \vec{i} V\end{aligned}$$

Then,  $E_x = E_z = 0$  and  $B_x = B_y = 0$ . Moreover, with the gas fully ionized  $f = 0$  and thus  $b = 0$ . Then, Eq. (III-4) may be simplified to

$$\begin{vmatrix} J_x \\ J_y \\ J_z \end{vmatrix} = \frac{\sigma}{1 + (\omega_e \bar{\tau}_e)^2} \begin{vmatrix} 1 & -\omega_e \bar{\tau}_e & 0 \\ \omega_e \bar{\tau}_e & 1 & 0 \\ 0 & 0 & 1 + (\omega_e \bar{\tau}_e)^2 \end{vmatrix} \begin{vmatrix} 0 \\ E' \\ 0 \end{vmatrix}$$

This is the same expression given by Sonnerup (Ref. 3), only a different orientation was used here.

TABLE 1  
NUMBER FRACTIONS OF EQUILIBRIUM NITROGEN

Gas Specie	$N_2$			$N_2^+^*$		
T, °K	p, atm			p, atm		
	$10^{-1}$	1	10	$10^{-1}$	1	10
2,000	1.00	1.00	1.00	$1.80 \times 10^{-18}$	$3.70 \times 10^{-19}$	$1.20 \times 10^{-19}$
2,500	1.00	1.00	1.00	$1.40 \times 10^{-14}$	$4.30 \times 10^{-15}$	$1.40 \times 10^{-15}$
3,000	1.00	1.00	1.00	$6.90 \times 10^{-12}$	$2.22 \times 10^{-12}$	$7.10 \times 10^{-13}$
3,500	0.9992	0.9997	0.9999	$6.30 \times 10^{-10}$	$2.00 \times 10^{-10}$	$6.30 \times 10^{-11}$
4,000	0.9944	0.9982	0.9994	$1.86 \times 10^{-8}$	$5.95 \times 10^{-7}$	$3.95 \times 10^{-9}$
6,000	0.4825	0.7925	0.9290	$1.71 \times 10^{-5}$	$1.16 \times 10^{-5}$	$5.25 \times 10^{-6}$
8,000	0.0115	0.0960	0.4120	$3.05 \times 10^{-5}$	$8.33 \times 10^{-5}$	$1.26 \times 10^{-4}$
10,000	$3.90 \times 10^{-4}$	$4.50 \times 10^{-3}$	$4.60 \times 10^{-2}$	$1.90 \times 10^{-5}$	$6.95 \times 10^{-5}$	$2.18 \times 10^{-4}$
13,000	$1.70 \times 10^{-6}$	$1.10 \times 10^{-4}$	$2.00 \times 10^{-3}$	$2.47 \times 10^{-6}$	$2.85 \times 10^{-5}$	$1.50 \times 10^{-4}$
15,000	$1.80 \times 10^{-8}$	$6.50 \times 10^{-6}$	$3.10 \times 10^{-4}$	$1.90 \times 10^{-7}$	$8.80 \times 10^{-6}$	$9.10 \times 10^{-5}$

\*Also number of electrons created by  $N_2$  ionization.



TABLE 1 (Concluded)

Gas Specie	N			N <sup>+</sup> *		
T, °K	p, atm			p, atm		
	10 <sup>-1</sup>	1	10	10 <sup>-1</sup>	1	10
2,000	2.84x10 <sup>-9</sup>	8.90x10 <sup>-10</sup>	2.85x10 <sup>-10</sup>	0.00	0.00	0.00
2,500	8.80x10 <sup>-7</sup>	2.80x10 <sup>-7</sup>	8.70x10 <sup>-8</sup>	0.00	0.00	0.00
3,000	4.32x10 <sup>-5</sup>	1.38x10 <sup>-5</sup>	4.30x10 <sup>-6</sup>	1.56x10 <sup>-14</sup>	1.60x10 <sup>-15</sup>	1.60x10 <sup>-16</sup>
3,500	7.00x10 <sup>-4</sup>	2.30x10 <sup>-4</sup>	7.20x10 <sup>-5</sup>	1.15x10 <sup>-11</sup>	1.70x10 <sup>-12</sup>	1.18x10 <sup>-13</sup>
4,000	5.60x10 <sup>-3</sup>	1.77x10 <sup>-3</sup>	5.60x10 <sup>-4</sup>	1.88x10 <sup>-9</sup>	1.95x10 <sup>-10</sup>	1.95x10 <sup>-11</sup>
6,000	0.5180	0.2080	0.0710	1.03x10 <sup>-4</sup>	1.70x10 <sup>-5</sup>	2.00x10 <sup>-6</sup>
8,000	0.9740	0.8990	0.5890	7.25x10 <sup>-3</sup>	2.18x10 <sup>-3</sup>	5.00x10 <sup>-4</sup>
10,000	0.8543	0.9467	0.9375	0.0727	0.0243	0.0073
13,000	0.2630	0.6290	0.8630	0.3690	0.1855	0.0670
15,000	0.0540	0.3060	0.6740	0.4730	0.3473	0.1623

\* Also number of electrons created by N ionization.

**TABLE 2**  
**TYPICAL VALUES OF  $\ell n \Lambda$  FOR NITROGEN**

a.  $S = 0$

$\ell n \Lambda$			
T, °K	p = 0.01 atm	p = 1.0 atm	p = 10 atm
2,000	18.31	17.32	16.82
3,000	12.35	11.36	10.87
4,000	9.41	6.53	7.68
6,000	6.35	5.56	5.17
8,000	5.17	4.20	3.76
10,000	4.65	3.56	3.08
13,000	4.70	3.15	2.59
15,000	4.93	3.12	2.47

b.  $S = 0.01$  percent Potassium

$\ell n \Lambda$			
T, °K	p = 0.01 atm	p = 1.0 atm	p = 10 atm
2,000	6.56	5.57	5.07
3,000	5.99	4.51	3.96
4,000	6.45	4.50	3.65
6,000	6.31	5.07	4.17
8,000	5.17	4.19	3.73
10,000	4.65	3.56	3.08
13,000	4.70	3.14	2.60
15,000	4.95	3.12	2.57

c.  $S = 1.0$  percent Potassium

$\ell n \Lambda$			
T, °K	p = 0.01 atm	p = 1.0 atm	p = 10 atm
2,000	5.56	4.58	4.09
3,000	4.51	3.46	2.97
4,000	4.51	2.98	2.43
6,000	5.37	3.27	2.36
8,000	5.11	3.76	2.83
10,000	4.64	3.50	2.91
13,000	4.70	3.14	2.58
15,000	4.93	3.12	2.46

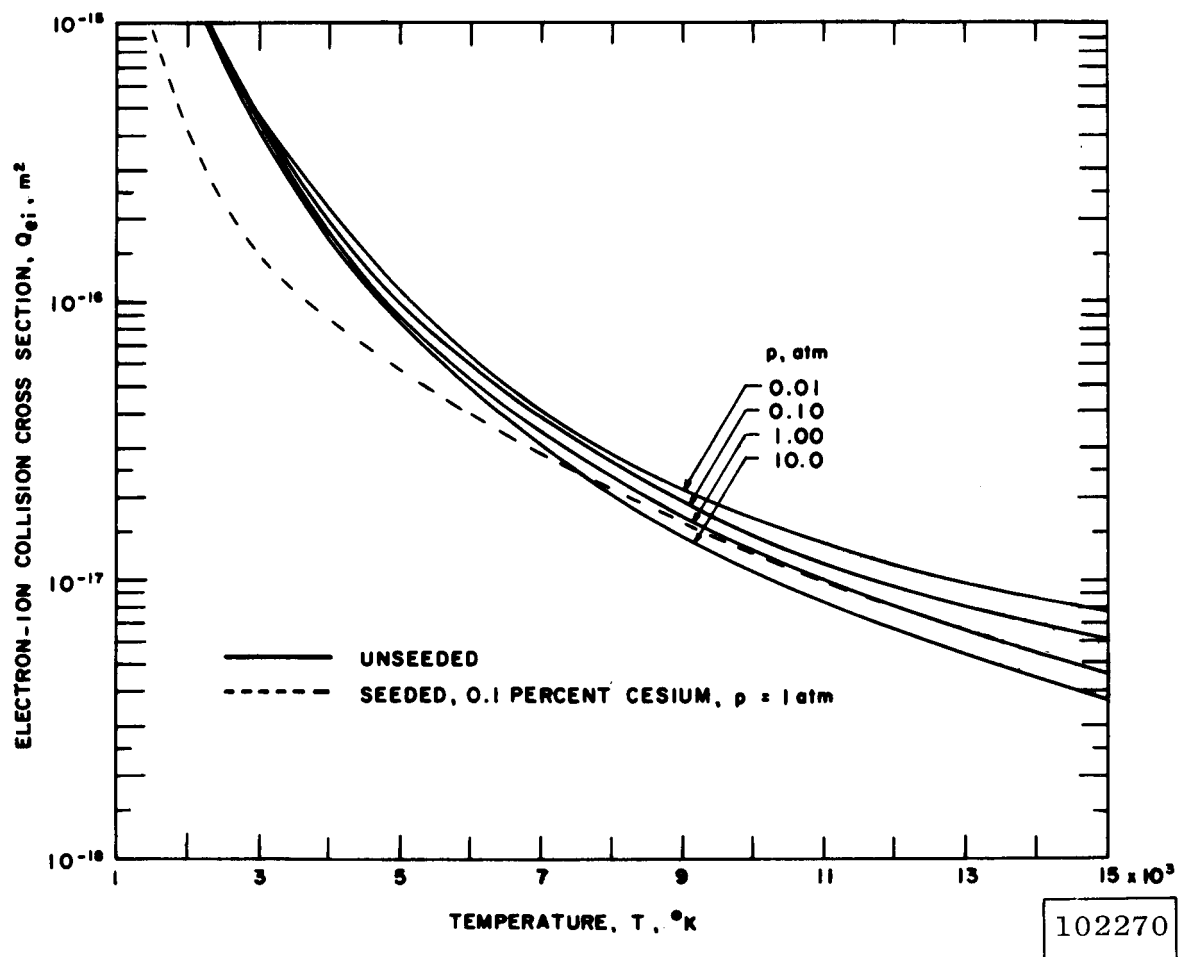


Fig. 1 Calculated Electron-Ion Collision Cross Sections for Argon

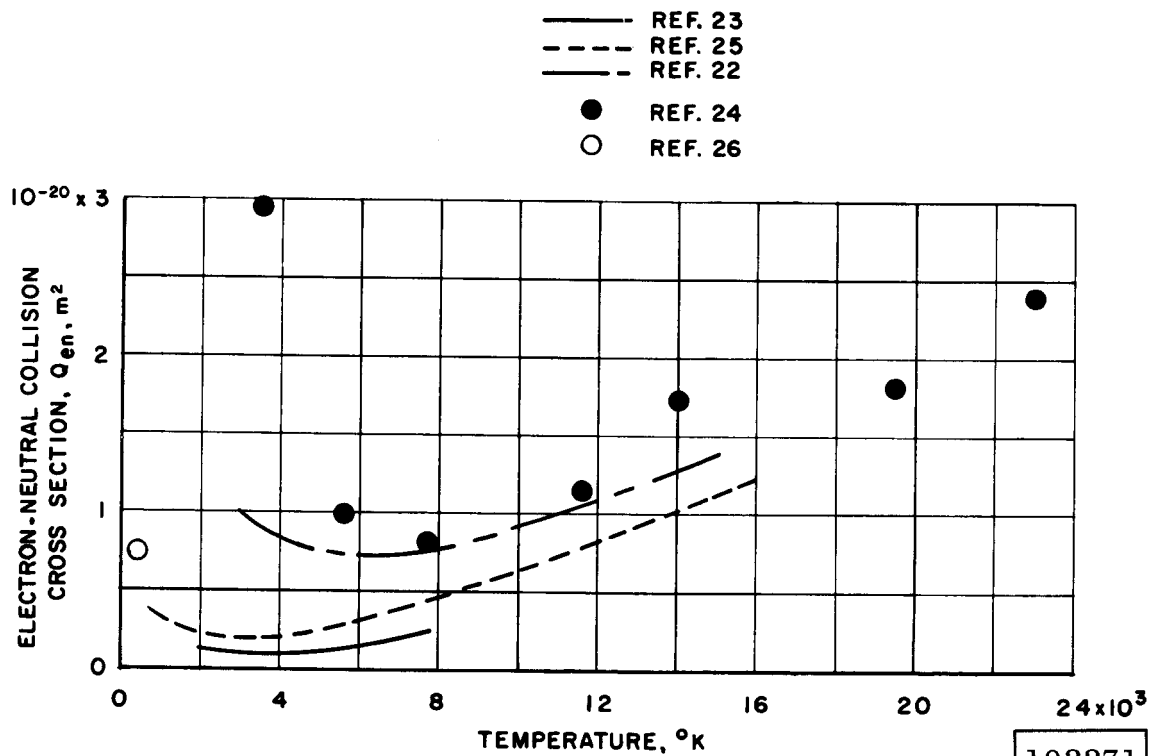
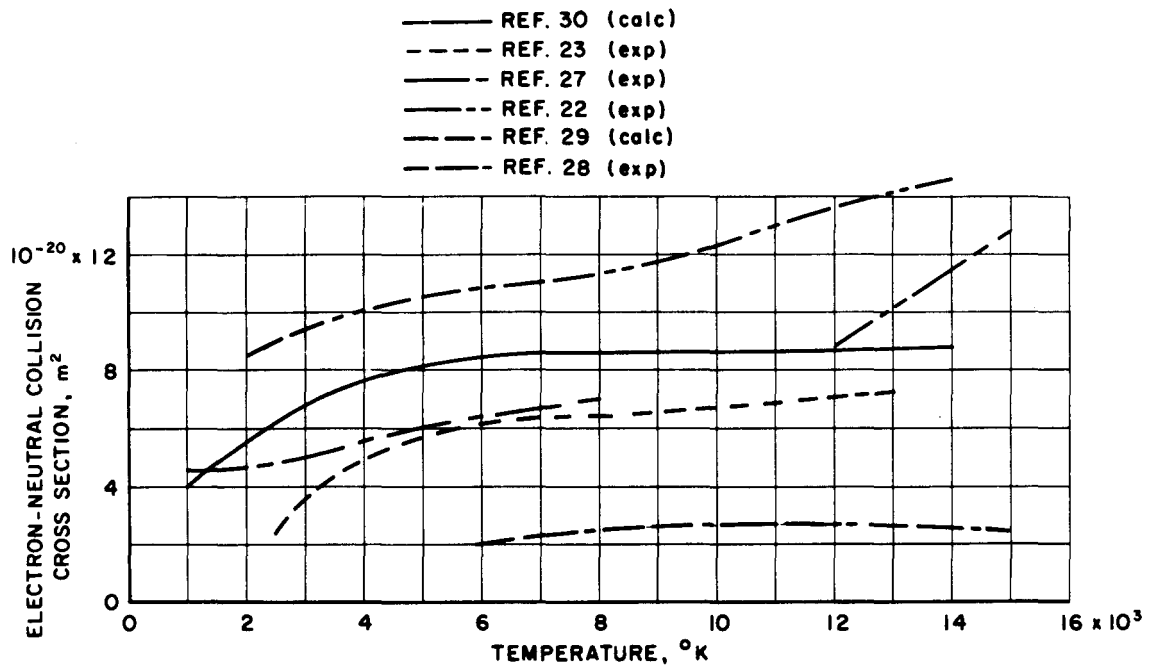
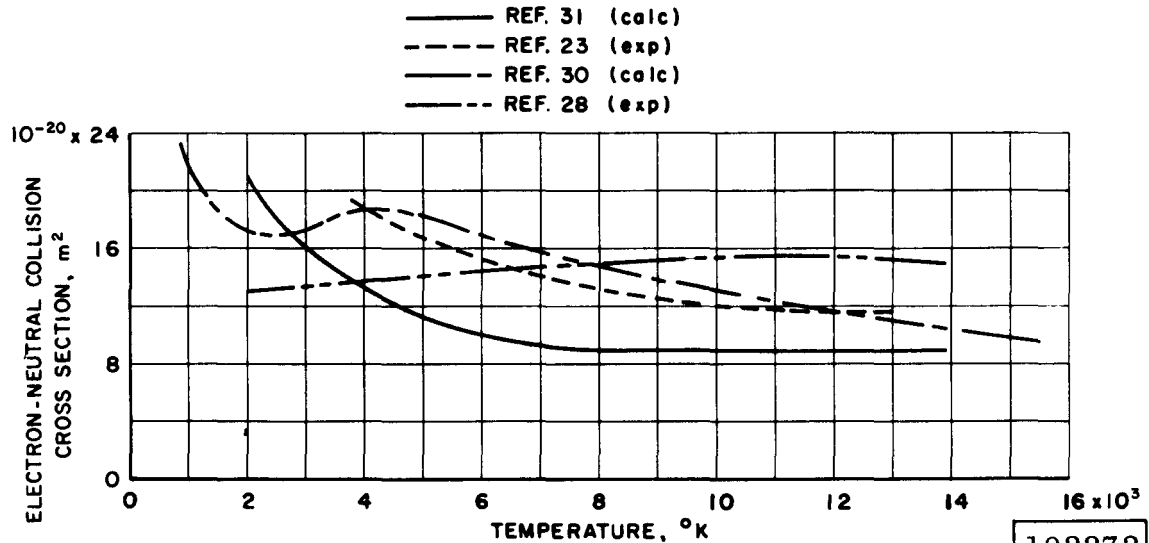


Fig. 2 Electron-Neutral Collision Cross Section for Argon

102271

a.  $N_2-e$ b.  $N-e$ 

102272

Fig. 3 Comparison of Collision Cross Sections for Nitrogen

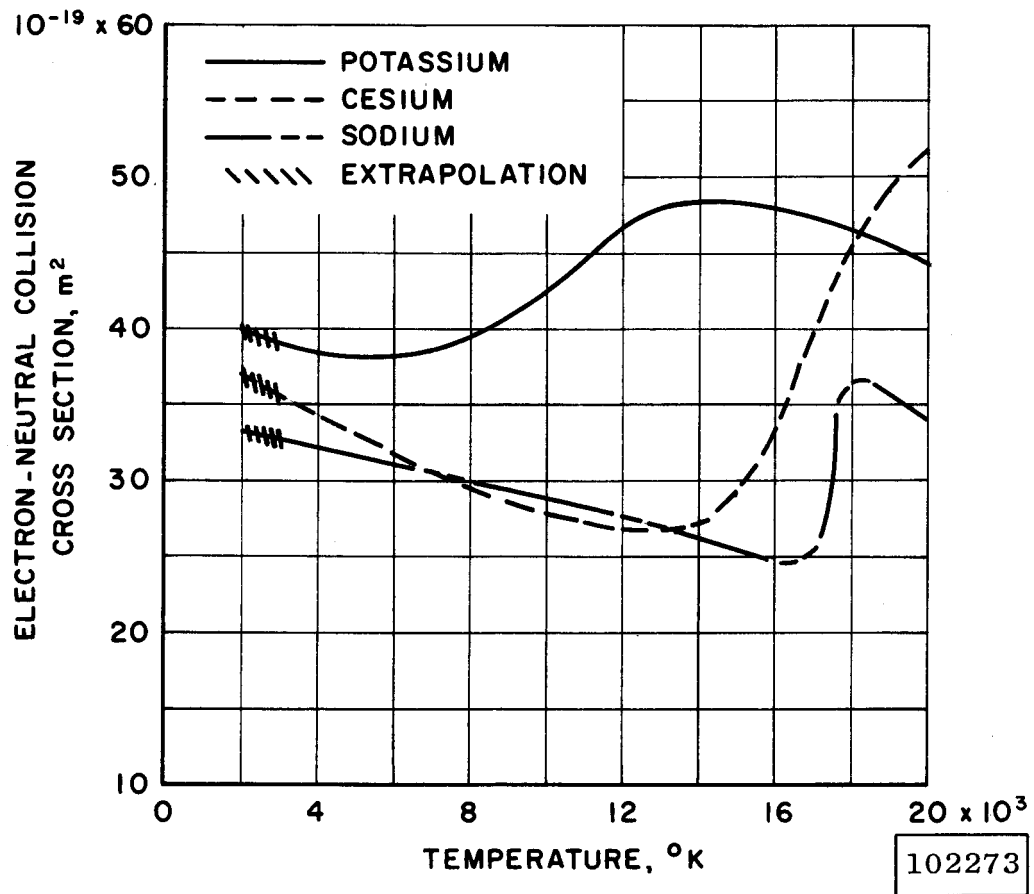


Fig. 4 Experimental Electron-Neutral Elastic Collision Cross Sections (Ref. 32)

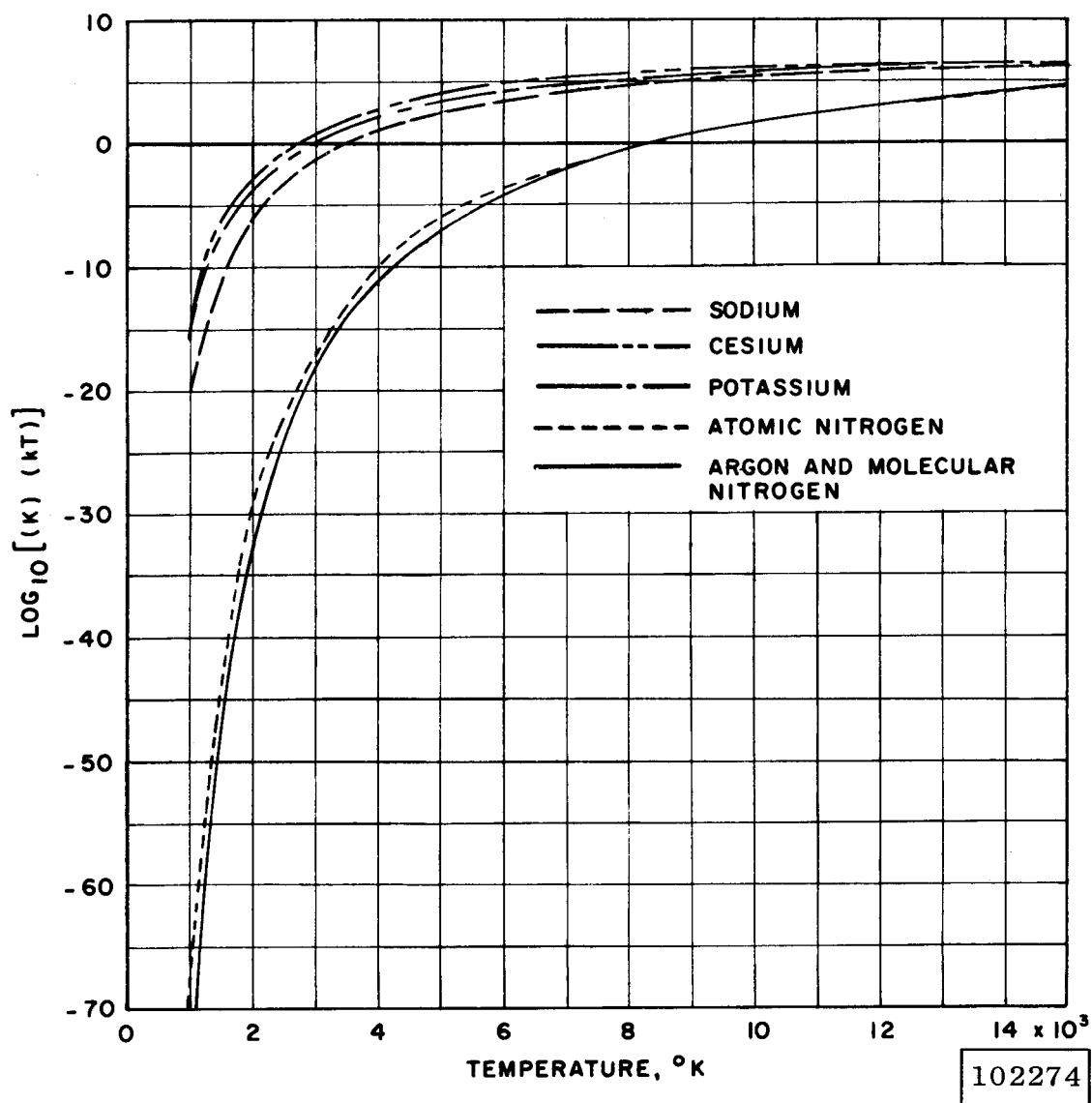
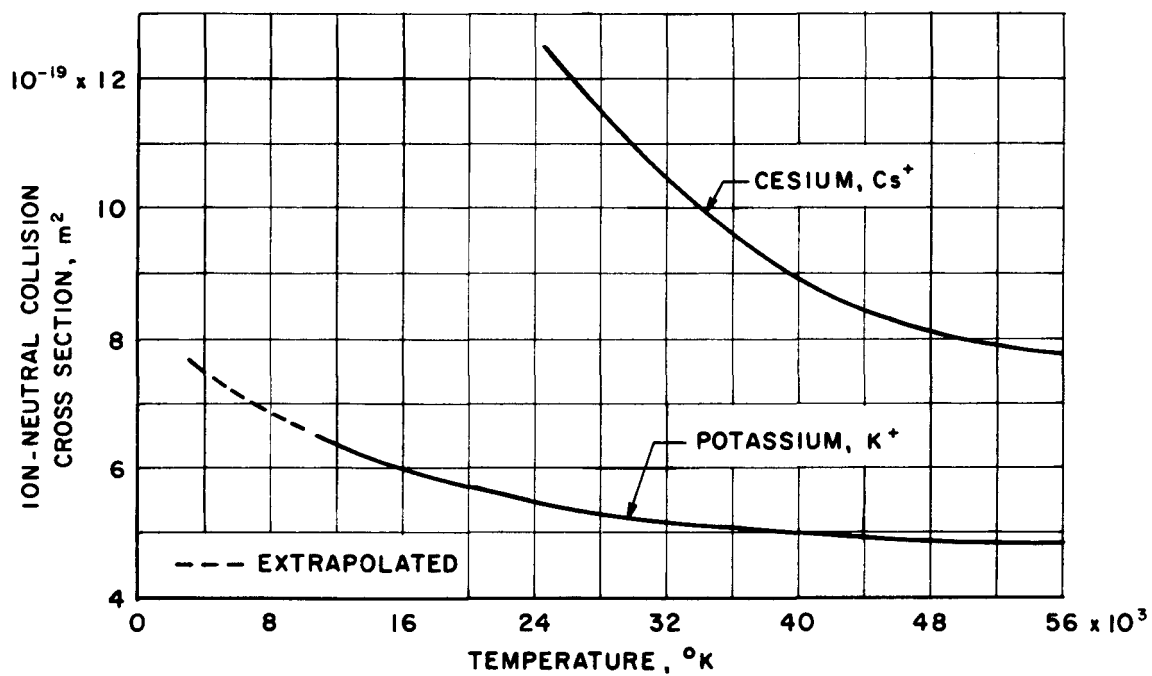
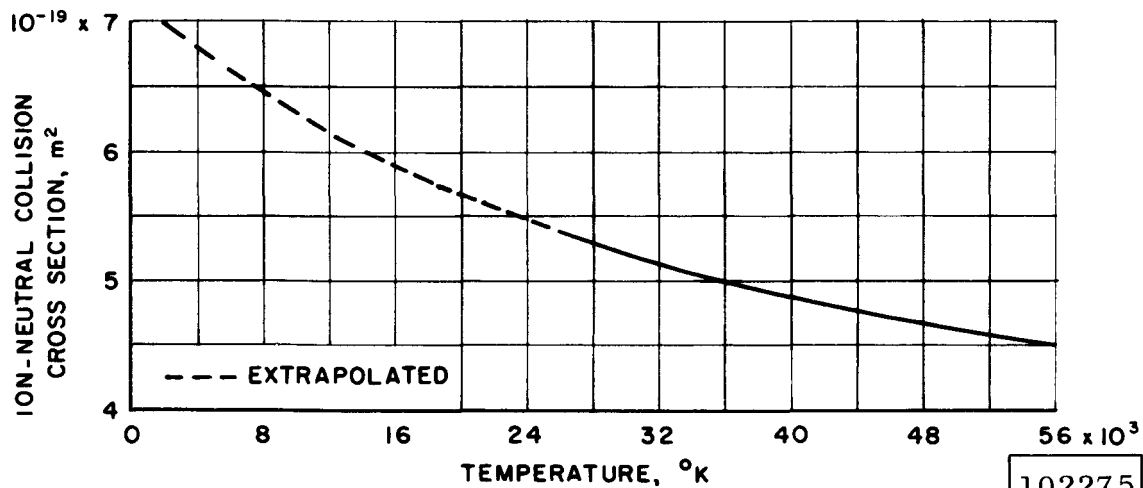


Fig. 5 Ionization Equilibrium Constant Function for Selected Elements



a. Ions in Argon

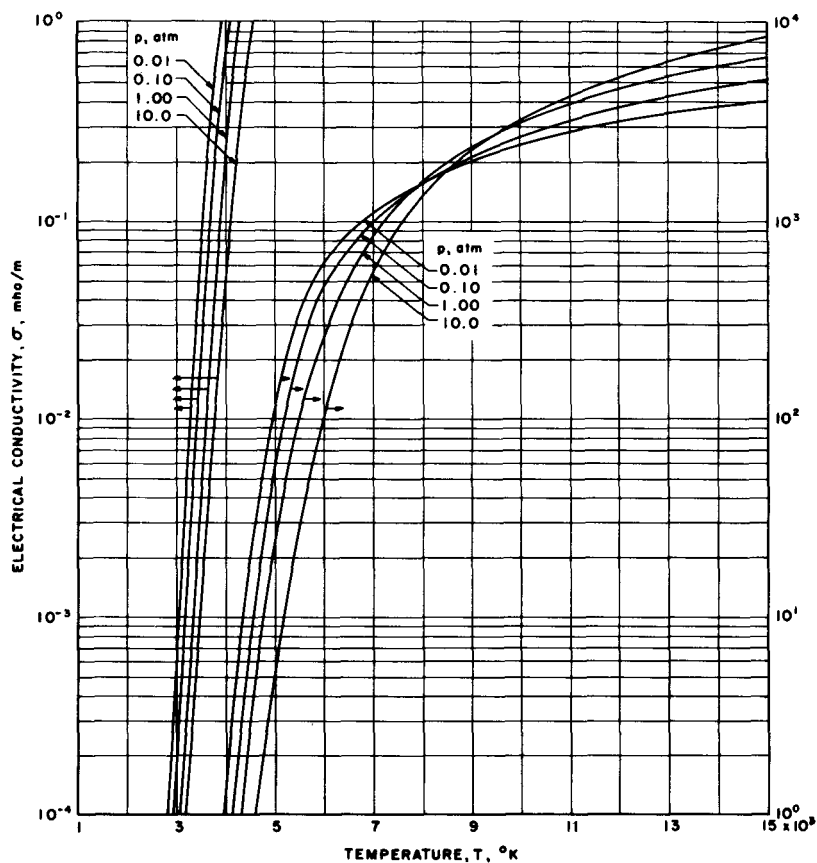


b. Potassium Ions in Nitrogen

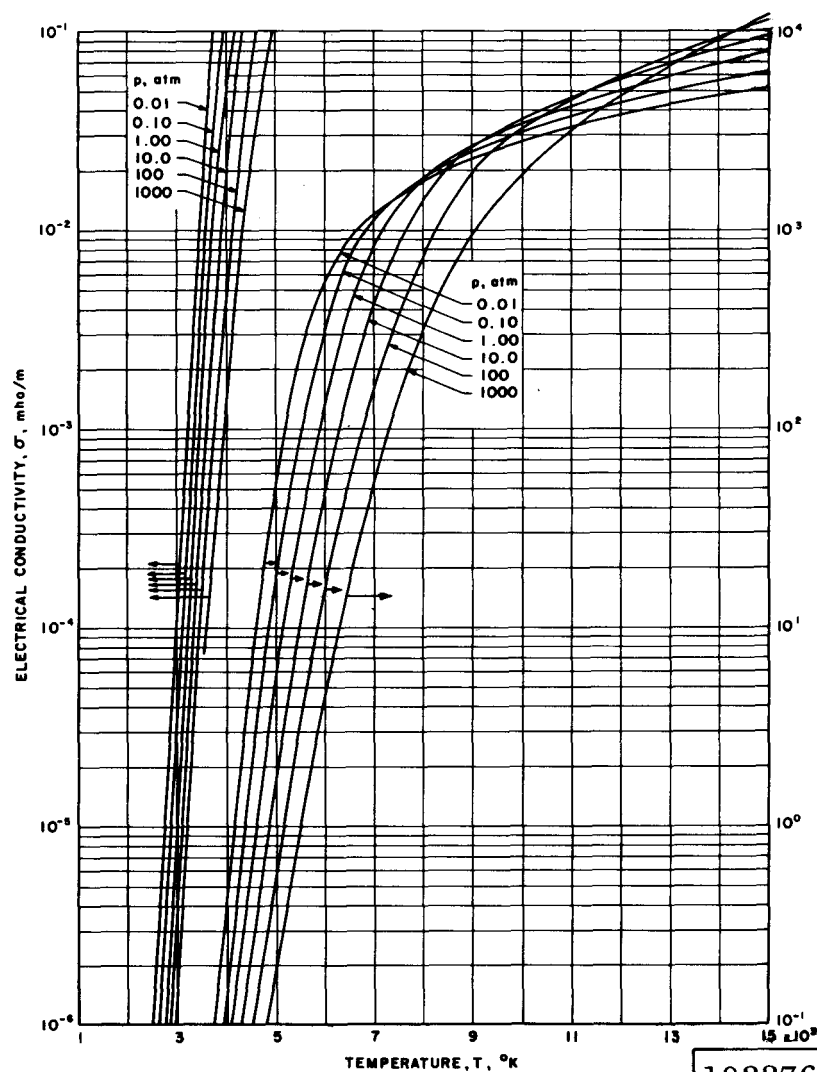
102275

Fig. 6 Experimental Ion-Neutral Collision Cross Sections for Various Substances (Ref. 22)





a. With Ref. 25 Cross Sections



b. With Ref. 22 Cross Sections

Fig. 7 Equilibrium Electrical Conductivities of Unseeded Argon

102276

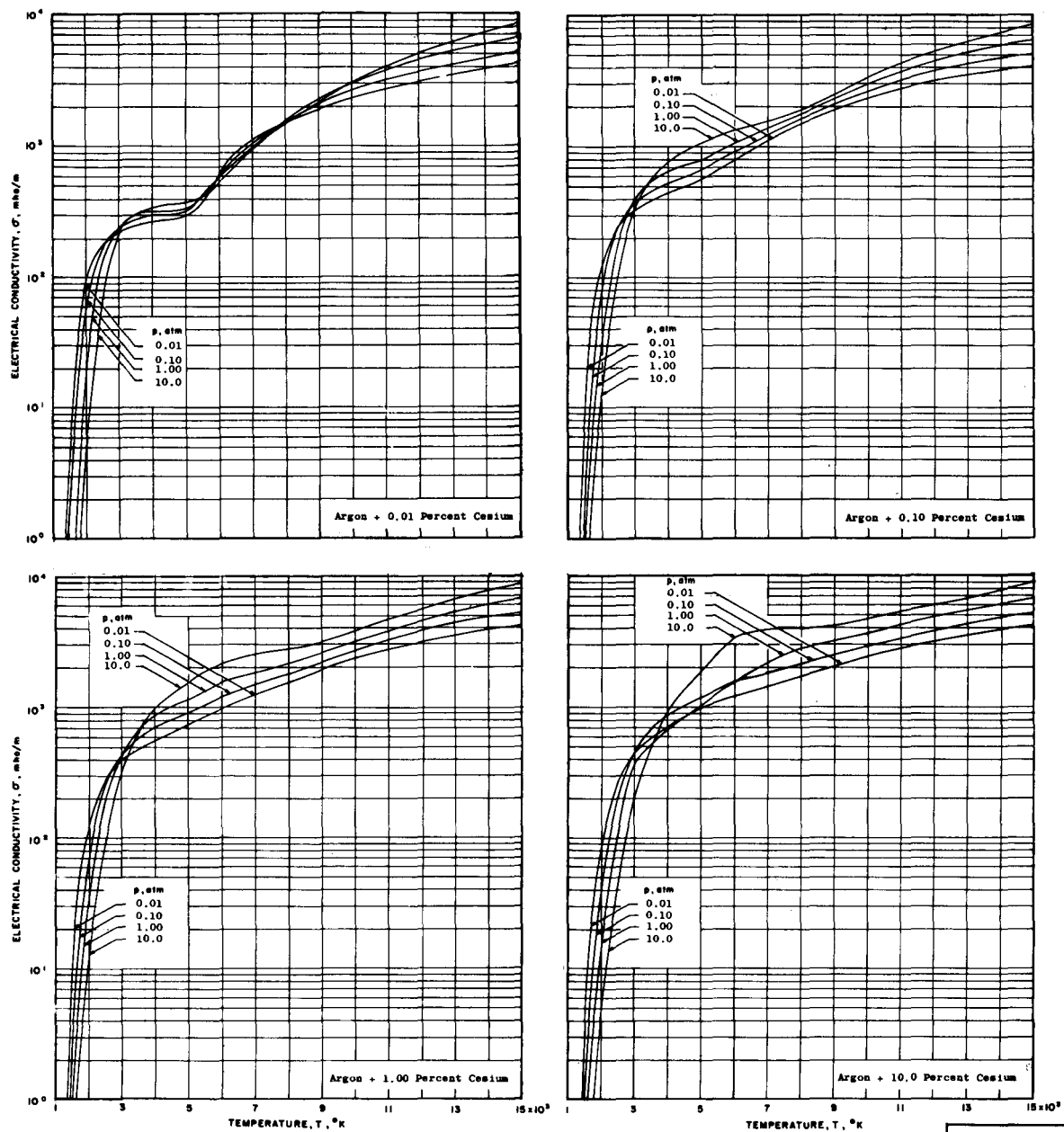


Fig. 8 Equilibrium Electrical Conductivity of Argon Seeded with Various Amounts of Cesium

102277

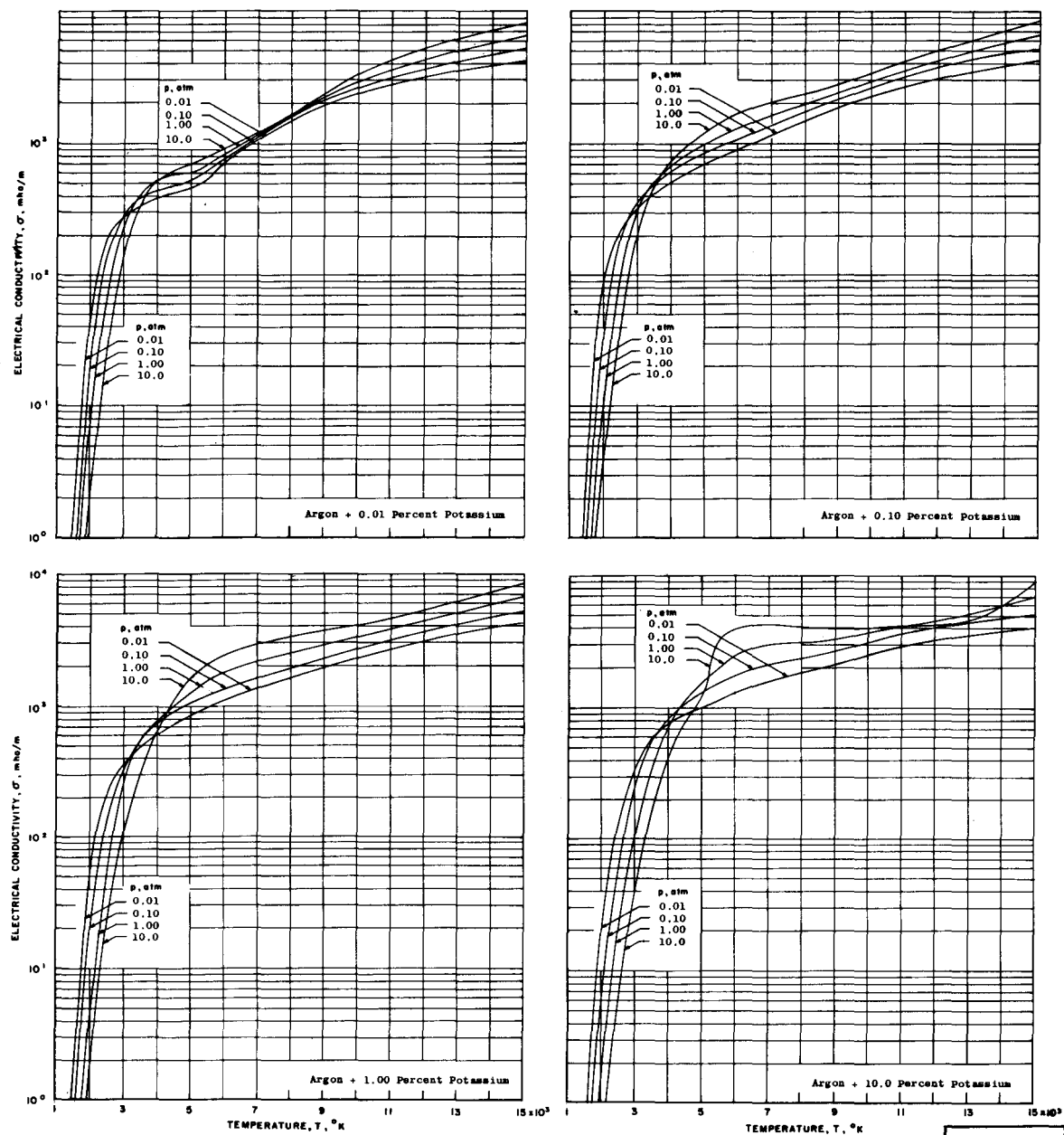


Fig. 9 Equilibrium Electrical Conductivity of Argon Seeded with Various Amounts of Potassium

102278

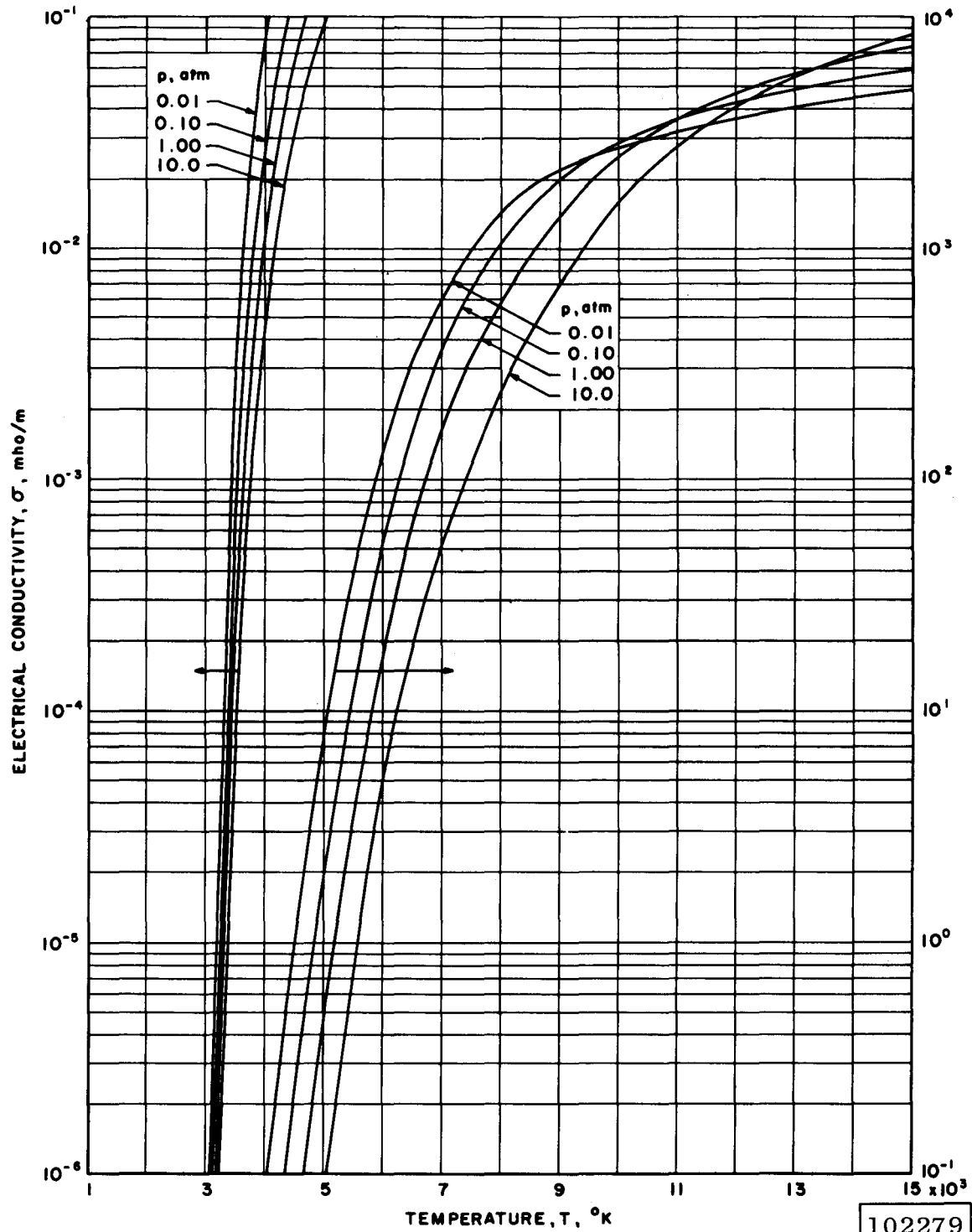


Fig. 10 Equilibrium Electrical Conductivity of Unseeded Nitrogen

102279

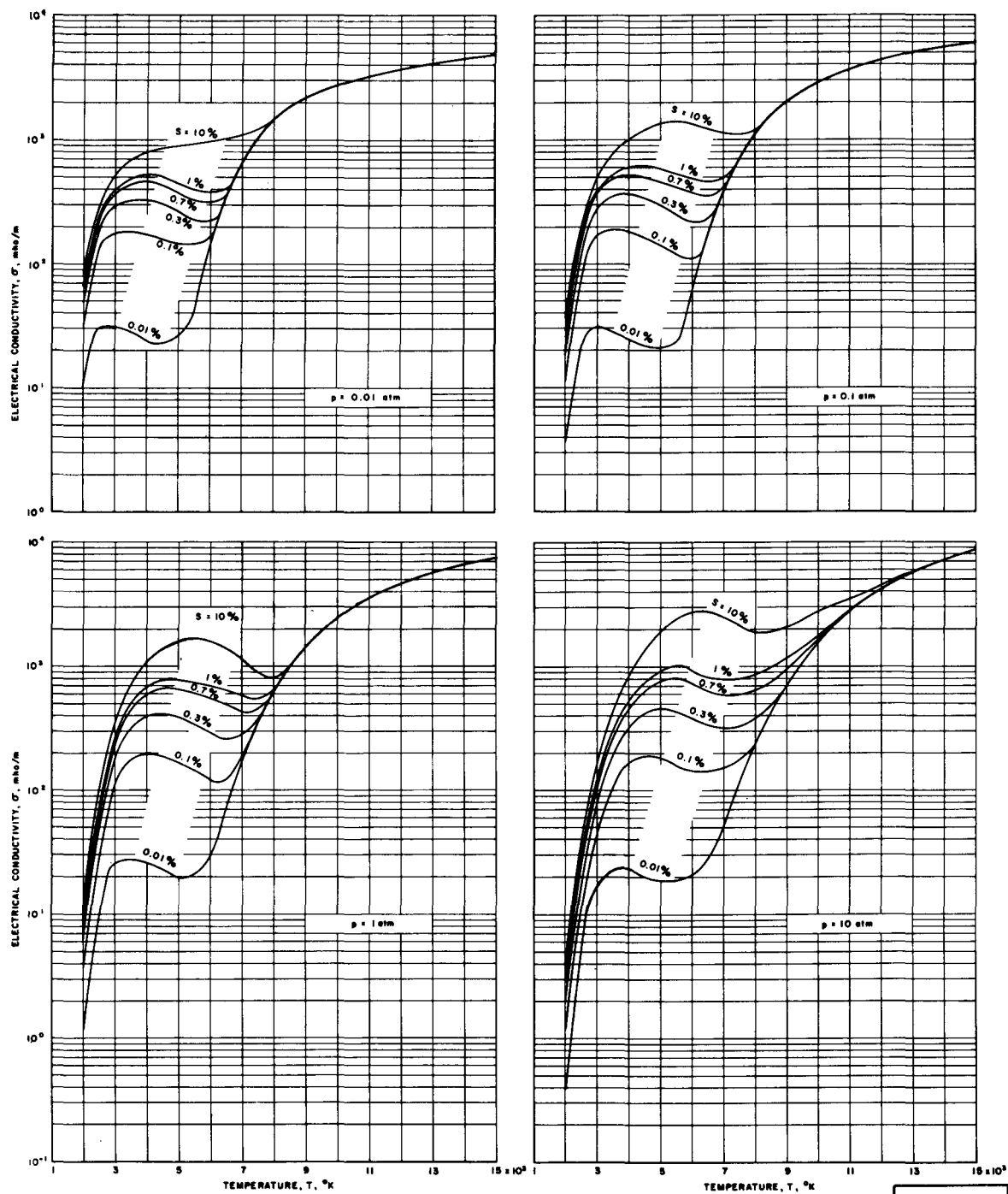


Fig. 11 Equilibrium Electrical Conductivity of Nitrogen Seeded with Various Amounts of Cesium

102280

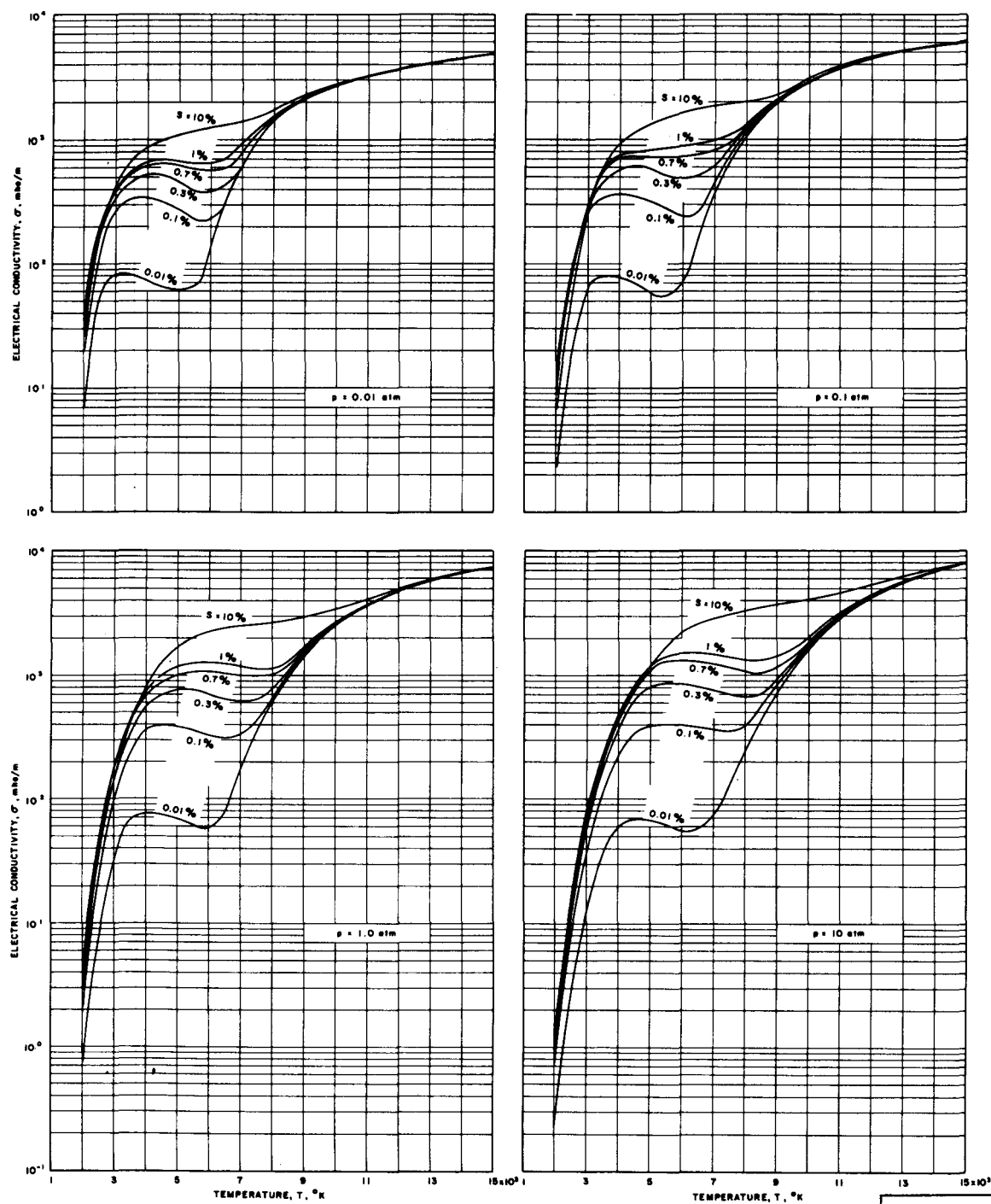


Fig. 12 Equilibrium Electrical Conductivity of Nitrogen Seeded with Various Amounts of Potassium

102281

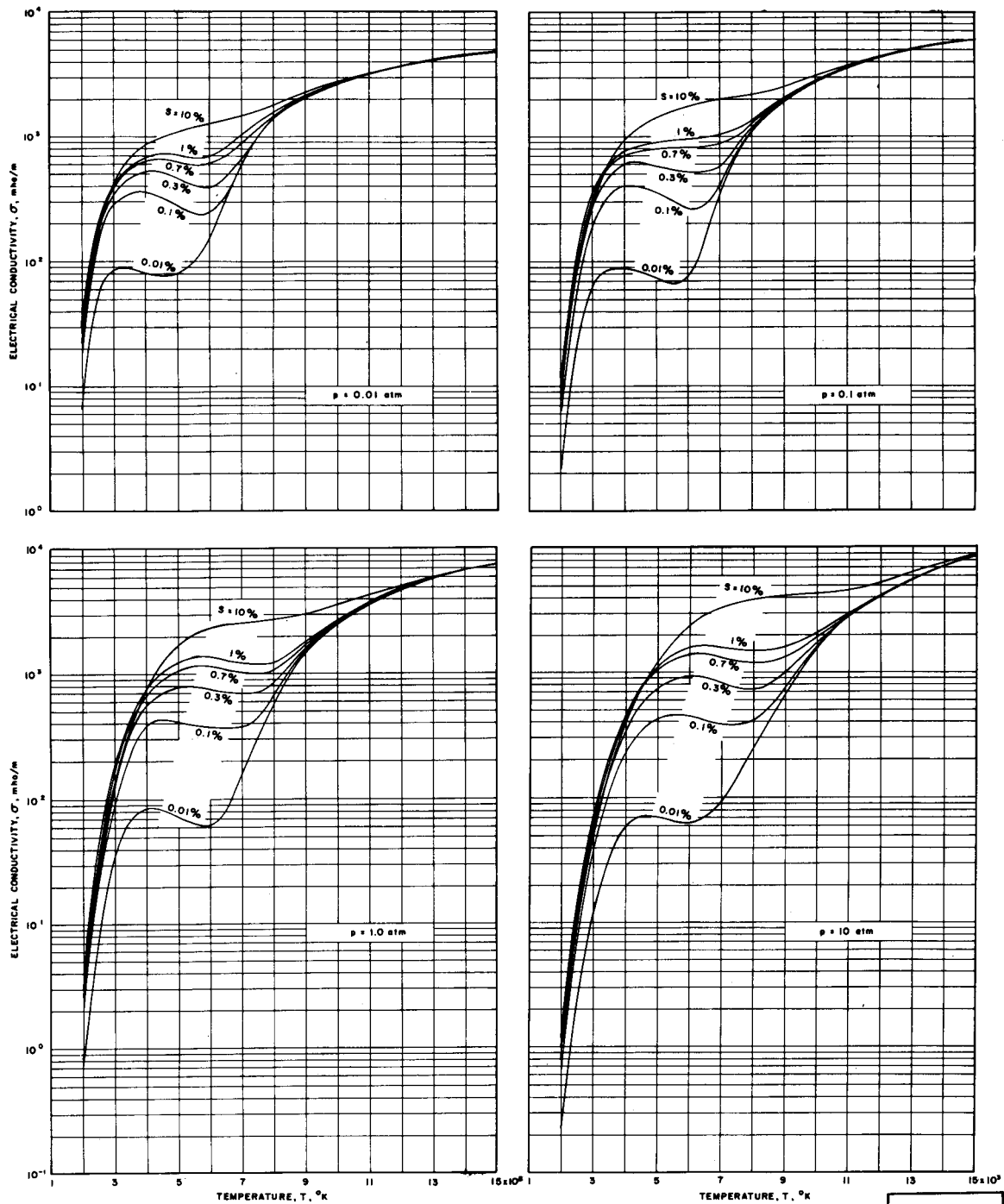
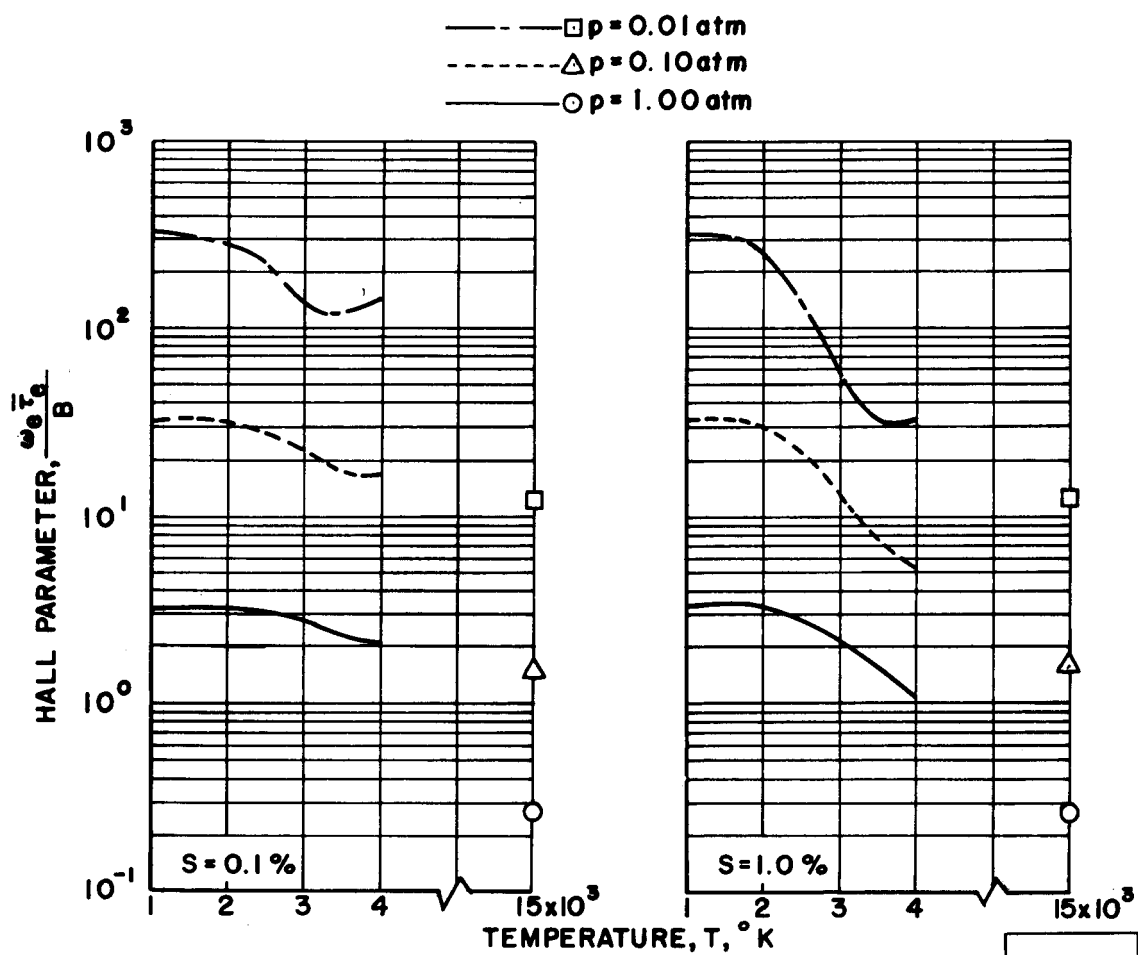


Fig. 13 Equilibrium Electrical Conductivity of Nitrogen Seeded with Various Amounts of NaK

102282

Fig. 14 Typical Values of the Hall Parameter,  $\omega_e \tau_e$



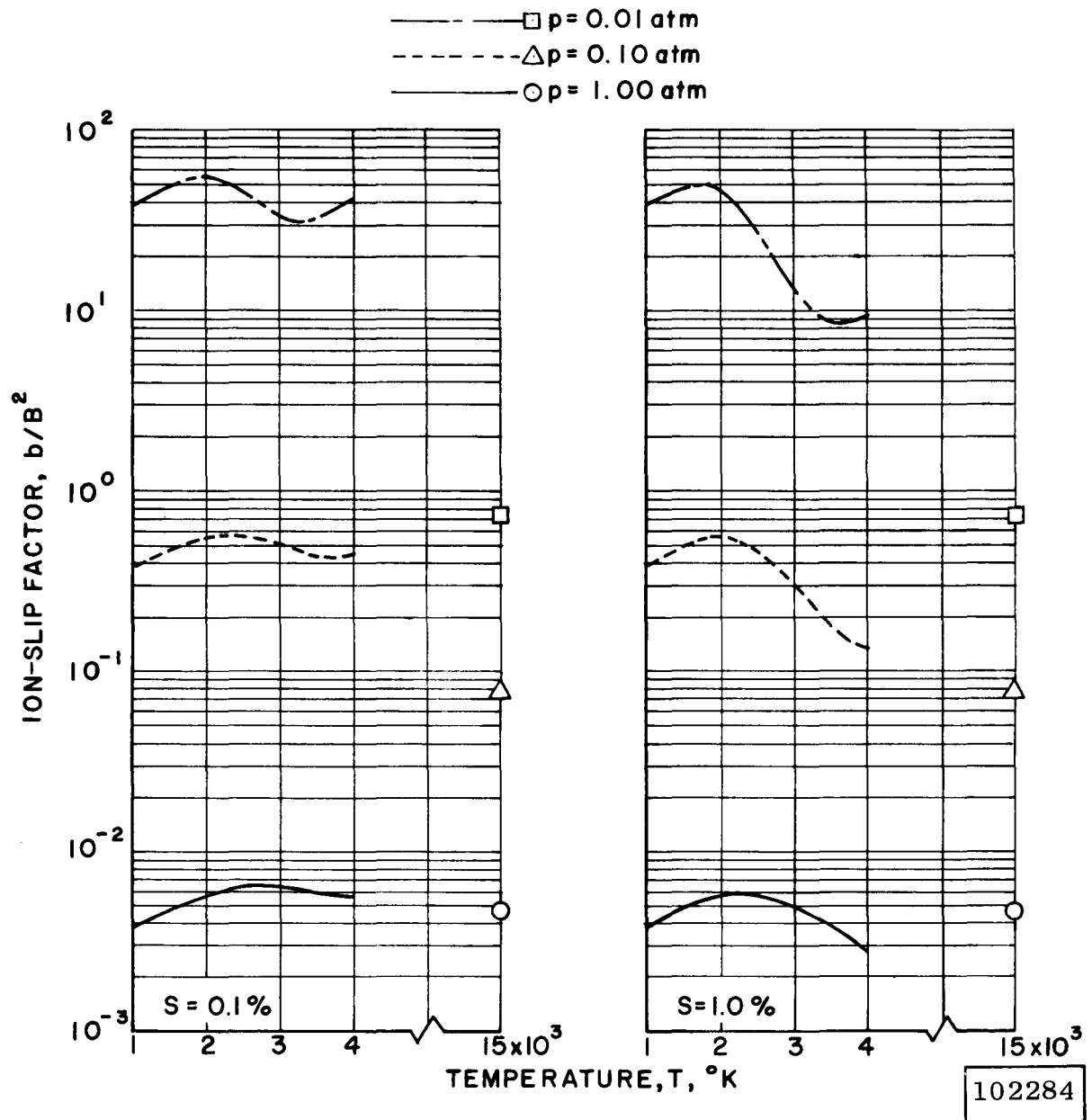


Fig. 15 Typical Values of the Ion-Slip Factor

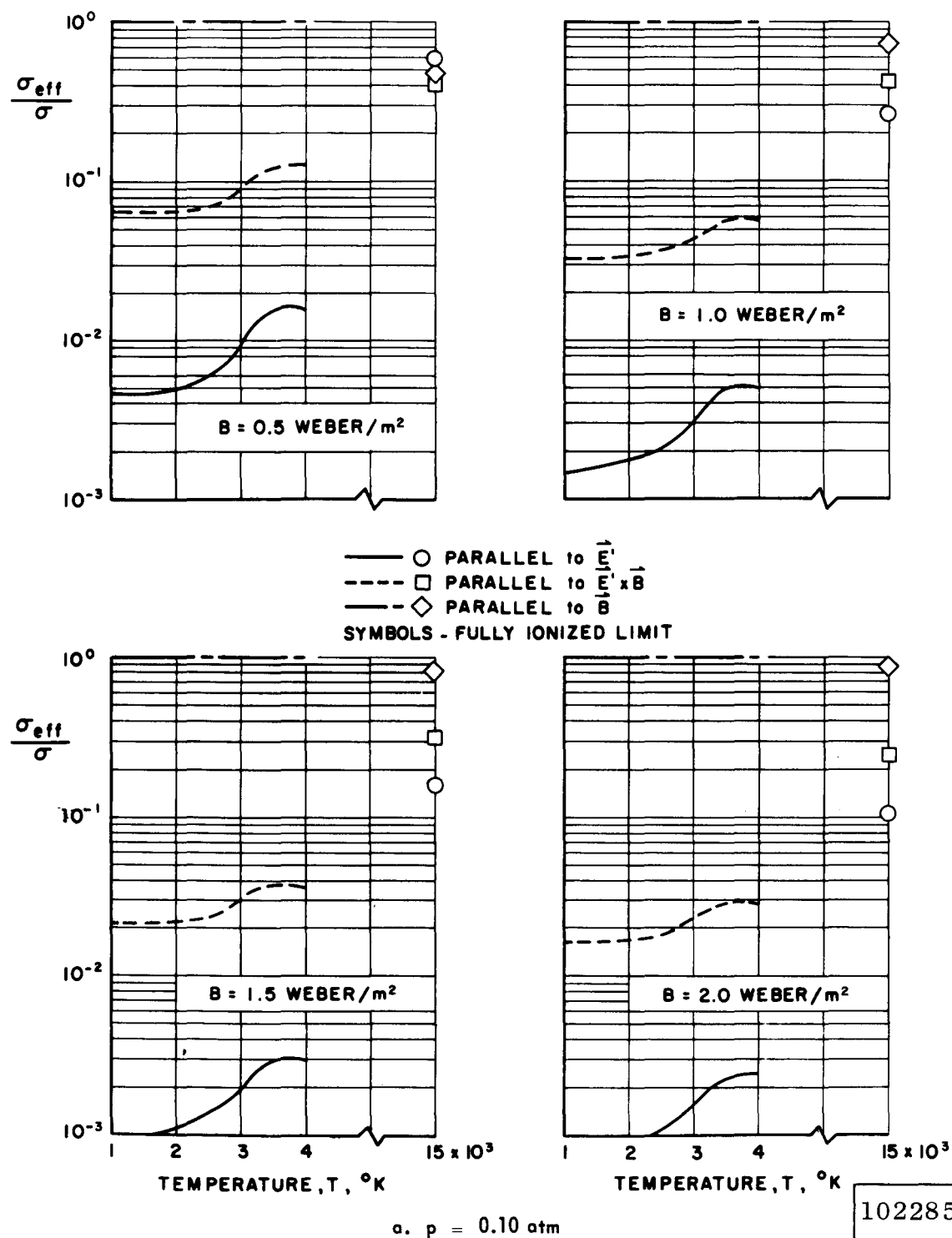


Fig. 16 Effect of a Magnetic Field on Electrical Conductivity of Nitrogen Seeded with 0.1 percent Potassium

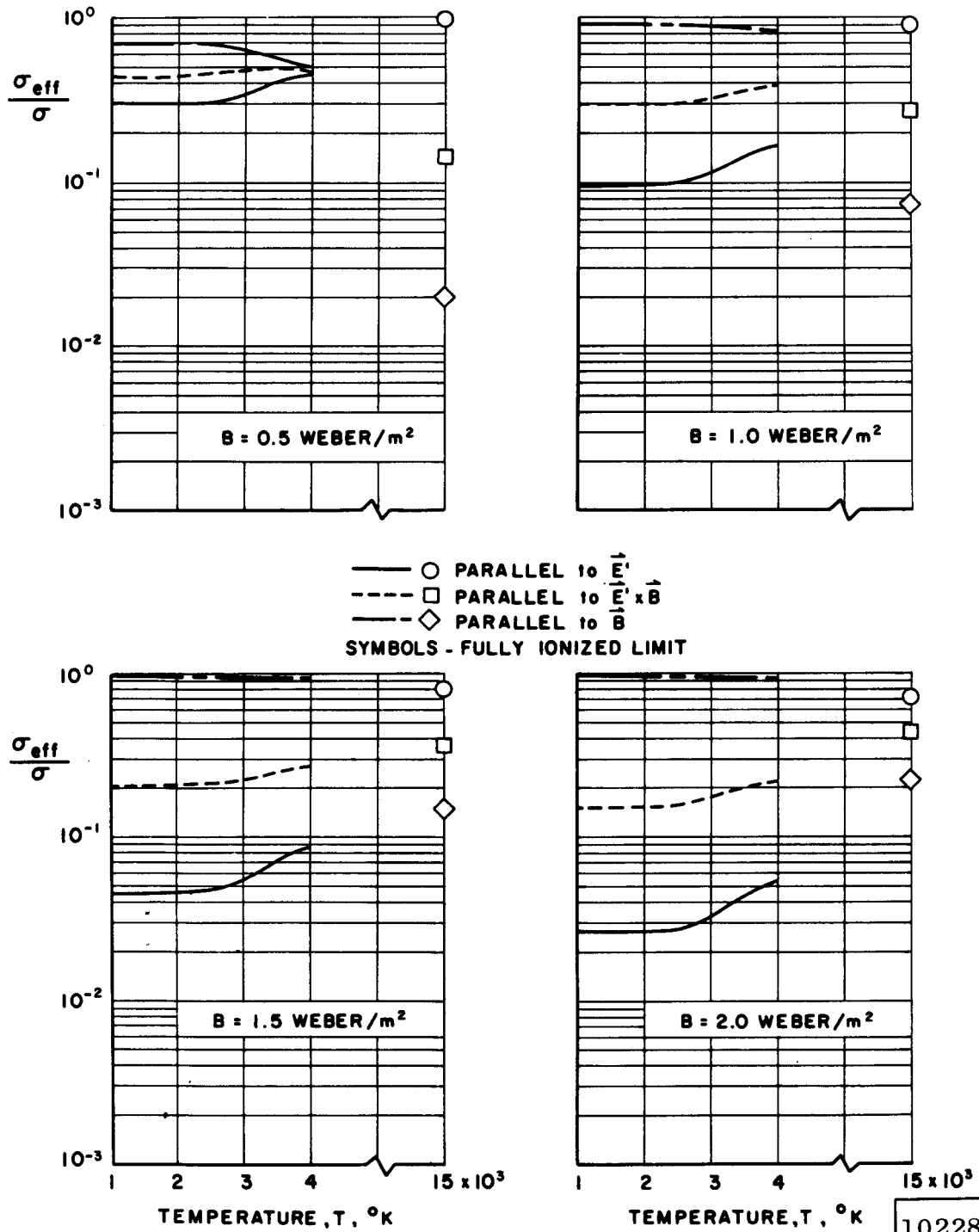
b.  $p = 1.00 \text{ atm}$ 

Fig. 16 Concluded

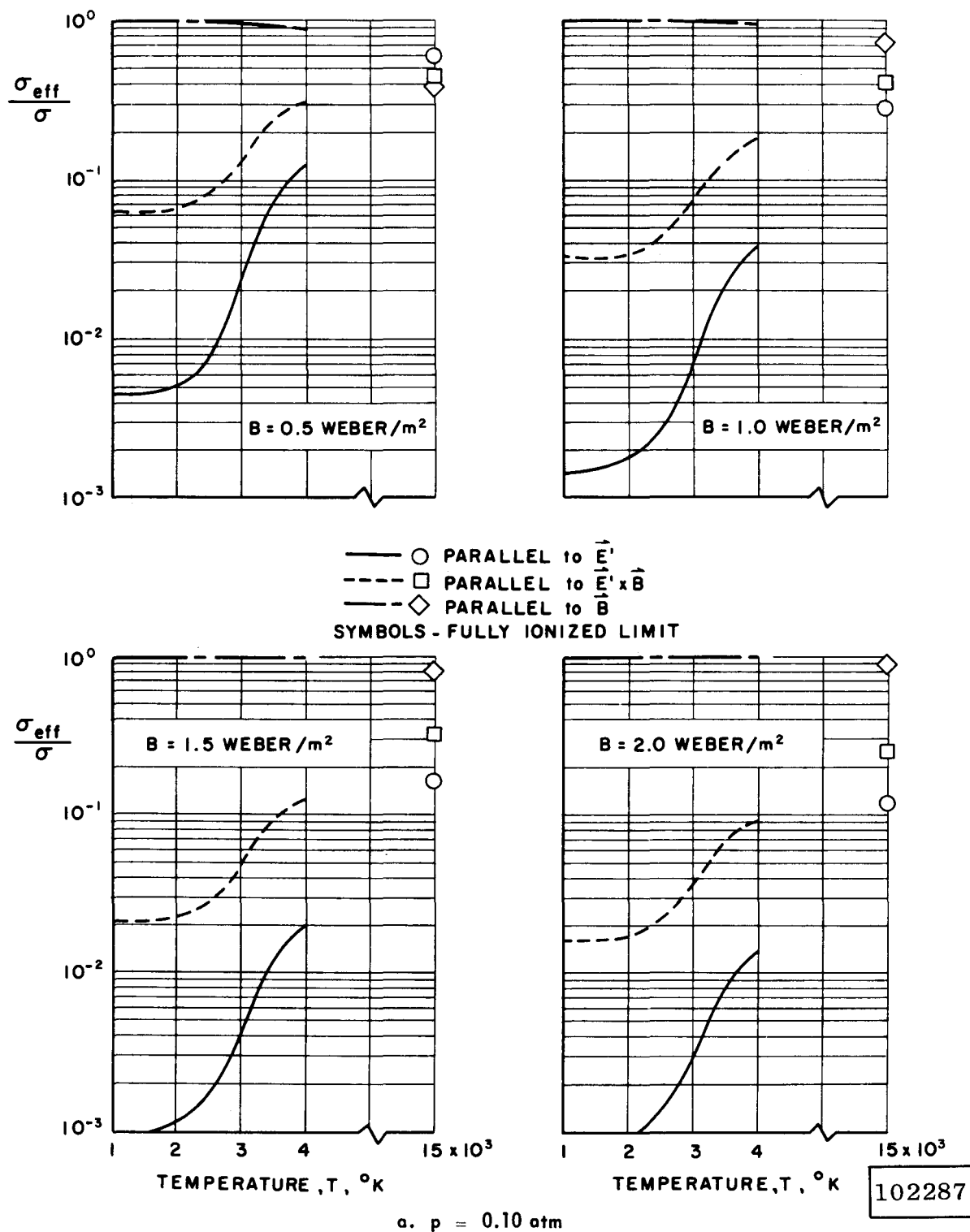


Fig. 17 Effect of a Magnetic Field on Electrical Conductivity of Nitrogen Seeded with 1.0 percent Potassium

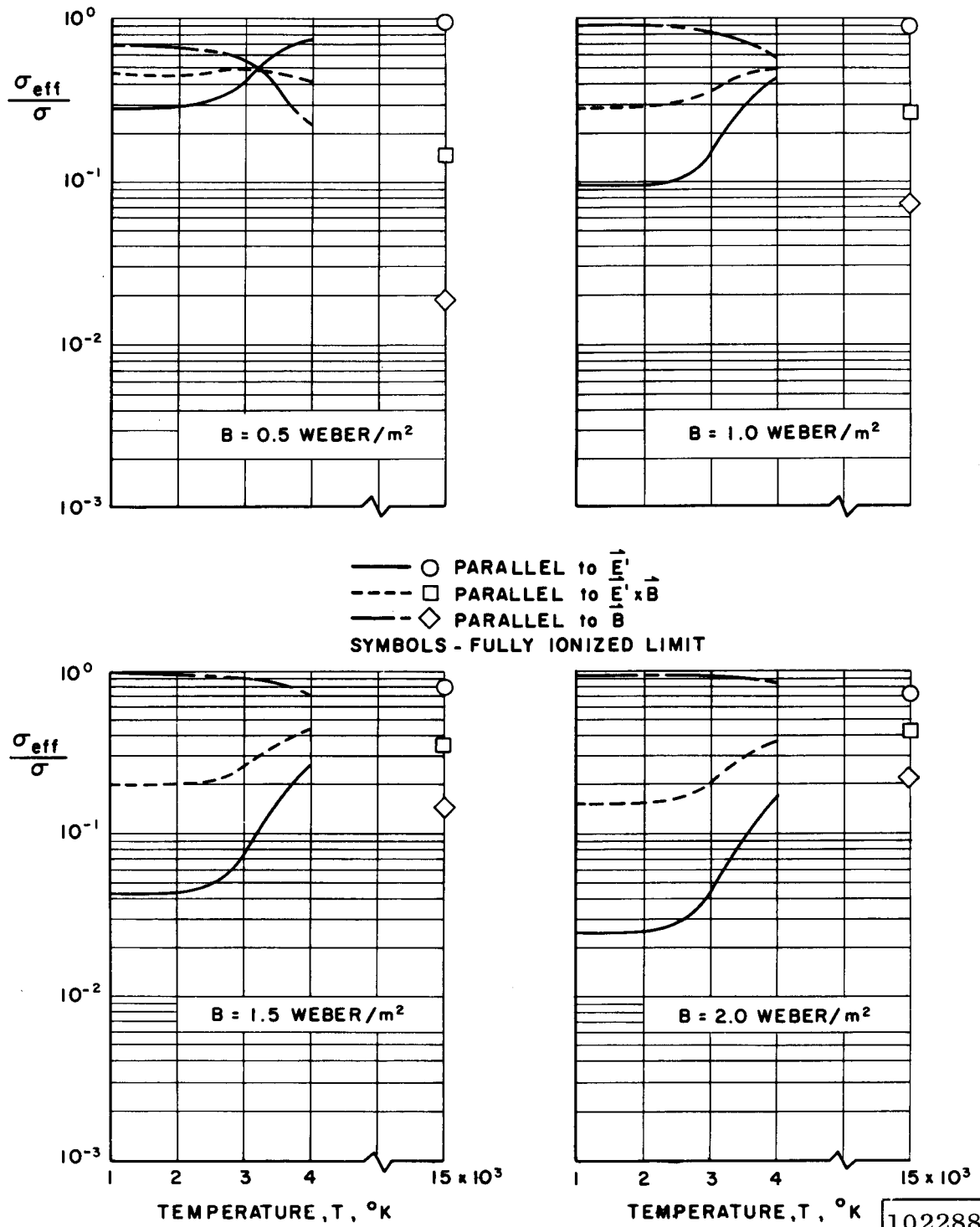
b.  $p = 1.00 \text{ atm}$ 

Fig. 17 Concluded